ROYAL SOCIETY OF CHEMISTRY

PERSPECTIVE

Check for updates

Multivalently engineered glyco-nanoplatforms for targeted therapy and diagnostics

Xiao-Lin Zhang,[a] Han Ding, [ID][a] Jia-Yi Zheng,[a] Hongzhi Cao[bc] and Xue-Wei Liu [ID] *[abc]

Glyco-nanoplatforms have emerged as powerful nanosystems that exploit glycan–lectin interactions for targeted therapy, diagnostics, and immunomodulation. By presenting glycans in multivalent architectures, glyco-nanoplatforms enhance binding affinity and specificity toward glycan-recognizing receptors on mammalian and bacterial cells. This perspective highlights recent advances in the design and synthesis of glyco-nanoplatforms across four key classes, including glyco-gold nanoparticles, glycopolymer-based nanoplatforms, glyco-functionalized quantum dots, and glycan-based magnetic nanocomposites. Through diverse synthetic strategies, structurally distinct glyco-nanoplatforms have been developed with improved binding affinities, stability, and biodistribution. Moreover, we further discuss their diverse biomedical applications in both mammalian and bacterial cells, ranging from targeted cancer therapy and biosensing to immunomodulation and antimicrobial treatment. Finally, we outline key challenges and provide an outlook on further directions in this field, aiming to unlock the therapeutic potential of the glyco-code.

[a]*School of Chemistry, Chemical Engineering and Biotechnology, Nanyang Technological University, Singapore 637371, Singapore. E-mail: xuewei@ntu.edu.sg*
[b]*Key Laboratory of Marine Drugs of Ministry of Education, Shandong Key Laboratory of Glycoscience and Glycotherapeutics, School of Medicine and Pharmacy, Ocean University of China, Qingdao 266003, China*
[c]*Laboratory for Marine Drugs and Bioproducts, Qingdao Marine Science and Technology Center, Qingdao 266237, China*

1 Introduction

Carbohydrates are ubiquitous and functionally diverse biomolecules whose precise spatial arrangement and composition encode a rich layer of biological information, referred to as the "glyco-code".[1,2] Beyond their role as essential nutrients, these glycans mediate a wide range of cellular communication and recognition. Through interactions with carbohydrate-binding proteins such as lectins, they regulate numerous pathophysiological processes, including cell differentiation, pathogen invasion, cancer progression, and immune dysfunction, positioning the glyco-code as a valuable blueprint for decoding disease mechanisms and advancing therapeutic innovation.[3,4] While glycan–lectin interactions are typically highly selective, their intrinsic monovalent affinities are

Dr Xiao-Lin Zhang received her BSc and MSc degrees in Food Science and Nutritional Engineering from China Agricultural University (2012–2018). Then she joined Prof. Xue-Wei's group at Nanyang Technological University (NTU), Singapore and obtained her PhD degree in Chemistry and Biological Chemistry in 2023. She is currently a Research Fellow in Liu's group at the School of Chemistry, Chemical Engineering and Biotechnology, NTU. Her research interests include glyco-code-based strategies for targeted drug delivery and antimicrobial intervention.

Xiao-Lin Zhang

Dr Han Ding received his BSc (2016) and MSc (2019) from Ocean University of China (OUC), where he investigated radical approaches in carbohydrate chemistry. He moved to Singapore in 2021 to join Prof. Xue-Wei's group at Nanyang Technological University (NTU) and completed his PhD in 2025. He is now a Research Fellow in the Liu lab, developing artificial carbohydrate-based biomolecular assemblies through integrated design, synthesis, and biological evaluation to advance carbohydrate science for human health.

Han Ding

relatively weak, often falling in the mM to μM range.[5] To overcome this limitation, nature employs a compensated strategy by presenting multiple glycan copies in the carbohydrate epitopes to enable multivalent engagement with several receptor sites.[6] This cooperative binding markedly enhances overall affinity and often improves specificity. Although the underlying molecular mechanisms of multivalent interactions remain incompletely understood, it is widely believed that clustering, rebinding, and chelation processes may act in concert to strengthen glycan–protein interactions.[5]

Building on this principle, glyco-nanoplatforms have been developed as powerful systems that can present glycans in a multivalent arrangement with different architectures, to enhance binding affinities to target biological receptors.[7] Various glycan-functionalized nanostructures have been explored in targeted cancer therapies,[8,9] immunomodulation,[10,11] biosensing,[12,13] and antimicrobial strategies (Fig. 1).[11] These investigations have deepened our insights into the primary factors that govern carbohydrate–lectin interactions. Beyond the degree of multivalency, factors such as glycan type, conjugating linker, and the size and morphology of glyco-nanoplatforms have been shown to play critical roles in modulating glycan–lectin interactions both *in vitro* and *in vivo*. Moreover, the dynamic adsorption of proteins onto nano-carriers, known as the protein corona, has been shown to markedly influence *in vivo* performance of glyco-nanoplatforms, including biodistribution and targeting accuracy.[14] Regulating the composition of the protein corona presents a valuable approach to improving the selectivity and therapeutic efficacy of glyco-nanoplatforms in biomedical applications.[15] In this perspective, we summarize recent progress in the synthesis of different types of glyco-nanoplatforms and discuss their applications in both mammalian and bacterial cells, including targeted cancer therapy, biosensing, immunomodulation, and antimicrobial treatment. These advances will push forward glyco-nanoplatforms as next-generation tools for clinical treatments.

2 Classes of glyco-nanoplatforms

Inspired by the intriguing advantages of glyco-decorated nanoplatforms, diverse glyco-nanosystems have been developed to probe carbohydrate–protein and carbohydrate–carbohydrate interactions. In general, four principal classes of glyco-nanoplatforms dominate the field, including glyco-gold NPs (glyco-AuNPs), glycopolymer-based nanoplatforms, glyco-functionalized quantum dots (glycodots), and glycan-based magnetic nanocomposites. Nonetheless, clinical translation remains hindered by synthetic complexity, scalability constraints, and inconsistent efficacy,[16,17] prompting continued refinement and optimization of glyco-nanoplatform design and fabrication. This section summarizes recent advances in their preparation to guide the development of more efficient glyco-

Jia-Yi Zheng

Jia-Yi Zheng is a PhD candidate at the School of Chemistry, Chemical Engineering and Biotechnology, Nanyang Technological University (NTU), Singapore, supervised by Prof. Xue-Wei Liu. Before moving to NTU, she earned dual BSc degrees in Food Science and Engineering and in Communication from China Agricultural University in 2022. Her research lies at the interface of biochemistry and immunology, focusing on mechanistic studies in glyco-immunology and their application to therapeutics.

Hongzhi Cao

Dr Hongzhi Cao is a Professor at Ocean University of China (OUC). He obtained his BSc (1997) and MSc (2000) degrees from Zhengzhou University and PhD (2004) from Shanghai Institute of Organic Chemistry (SIOC), Chinese Academy of Science (CAS). From 2005 to 2009, he was a post doc fellow at the University of California at Davis. In 2010, He joined Shandong University as an associate professor and was later promoted to full professor. Since 2020, he has been a distinguished professor at the School of Pharmaceutical Science, OUC. His group develops novel strategies for enzymatic or chemoenzymatic synthesis of complex carbohydrates.

Xue-Wei Liu

Dr Xue-Wei Liu is a Professor at Nanyang Technological University (NTU), Singapore. He received his BSc and MSc degrees from China Agricultural University and his PhD degree from the University of Southern California. Between 2000 to 2003, he worked at Procter & Gamble (USA) and Chugai Pharmaceutical Co., Ltd (USA). He then conducted postdoctoral research at California Institute of Technology from 2003 to 2005. In 2006, he joined NTU as an assistant professor, subsequently being promoted to associate professor and then full professor. His research focuses on glycoscience, including synthetic carbohydrate chemistry, chemical glycobiology, and glyco-based drug discovery.
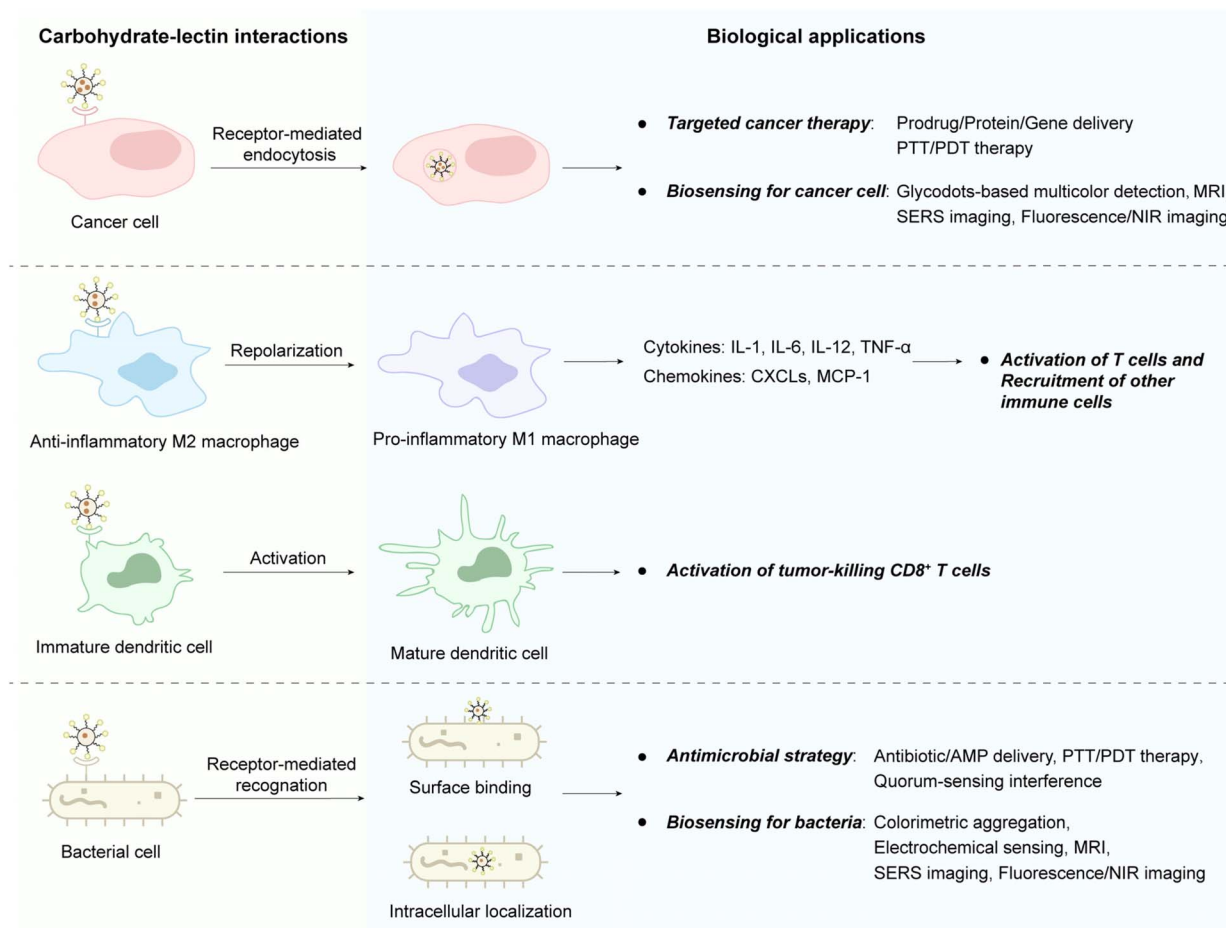
Fig. 1 Glyco-nanoplatforms enable diverse biological applications *via* specific carbohydrate−lectin interactions, including targeted cancer therapy, biosensing, immunomodulation, and antimicrobial strategies. In cancer therapy, glyco-nanoplatforms enter tumor cells *via* receptor-mediated endocytosis and release payloads such as prodrugs, proteins, or DNA/RNAs to induce cell death. Light-responsive agents further support photothermal (PTT) or photodynamic (PDT) therapy, either alone or in combination with chemo- or immunotherapies. For biosensing applications, glyco-nanoplatforms enable the detection of cancer cells or pathogens by different techniques, depending on the nanomaterial composition, including glycodots-based multicolor detection, magnetic resonance imaging (MRI) using magnetic nanocomposites, surface-enhanced Raman spectroscopy (SERS) *via* metallic nanostructures, as well as fluorescence/near-infrared imaging, colorimetric aggregation, and electrochemical sensing. For immunomodulation, they activate dendritic cells or repolarize anti-inflammatory M2 macrophages into pro-inflammatory M1 phenotypes, reshaping the immune microenvironment to enhance T cell-mediated clearance of tumor cells or bacteria. In antimicrobial strategies, glyco-nanoplatforms recognize bacterial surface lectins or enter cells *via* ATP-dependent ABC transporter commonly reported in glyco-based gold nanoparticles. Combined therapies, such as PTT coupled with antimicrobial agents, disrupt bacterial membranes, compromise cell integrity, and promote intracellular drug delivery. Moreover, quorum-sensing interference suppresses biofilm formation and virulence factor expression by mimicking inducers or blocking quorum-sensing receptors.

nanoplatforms. Table 1 illustrated various glyco-nanoplatforms with their biological applications or improved system features.

2.1 Glyco-gold nanoparticles

For decades, gold nanoparticles (AuNPs) have attracted substantial interest for biomedical applications due to their desirable features,[18] such as chemical inertness, stability, unique nanoscale optical/electronic properties, and readily tunable morphology.[19,20] Harnessing these attributes, AuNPs have been explored extensively as potential therapeutic and diagnostic platforms in cancer diseases,[21] immunomodulation,[22] and bacterial infections.[23] Though they possess these distinctive advantages, AuNPs still perform suboptimally *in vivo*.[24]

Specifically, once recognized as exogenous molecules, AuNPs trigger the immune system and are rapidly removed from the bloodstream, which causes poor biodistribution and shortened circulation time. To overcome these limitations, surface glyco-functionalization offers a practical strategy. By displaying glycans, glyco-AuNPs appear more "self-like" to the host immune system. The resulting increase in immune tolerance can enhance the biocompatibility and prolong circulation of glyco-AuNPs,[25] thereby improving the target delivery efficiency.

Carbohydrate-functionalized AuNPs have attracted growing interest due to their promising applications in biomedical nanotechnology.[26,27] The primary approach for anchoring carbohydrates onto AuNPs involves covalent attachment through bond formation with the metal surface, most

Table 1 Summary of diverse glyco-nanoplatform types and their associated biological applications or improved system features

Glyco-nanoplatform types		Applications/improved features	Ref.
Glyco-gold nanoparticles (glyco-AuNPs)	Ultra-small thiolated glyco-AuNPs by *in situ* reduction	Modeling cell surface interactions to study carbohydrate self-recognition First preparation of glyco-AuNPs	29
	Glucose-based ultra-small AuNPs	Drug delivery of ciprofloxacin against *Plasmodium falciparum* (*P. falciparum*)	31
	Ultra-small thiolated glyco-AuNPs	First photo-induced microfluidic strategy for reproducibility and precise control over particle size and morphology	34
	Mannose-stabilized AuNPs by post ligand exchange	Rapid, quantitative colorimetric detection of lectin	36
	Glycosaminoglycan-anchored AuNPs	Stem cell neural differentiation	38
	Glyco thiolate-capped AuNPs	Cytotoxicity in peripheral blood mononuclear cells (PBMCs) and A549 cancer cells	39
	N-Acetylneuraminic acid-functionalized AuNPs	Detection and capture of SARS-CoV-2	40
	Liposomal hyaluronic acid (HA)-AuNPs	Surface-enhanced Raman spectroscopy (SERS) imaging for tumor visualization and surgical guidance	41
	Star-shaped glycopeptide-capped glyco-AuNPs	Enhanced immune response for glyco-vaccine development	42
	Spherical mannose- or sialic acid-functionalized AuNPs	Functional polarization of liver macrophages Highly reproducible *via* a microfluidic strategy	44
Glycopolymer-based nanoplatforms	Amphiphilic PMAG-*b*-P(Lys-*co*-Phe) self-assembled spherical glycopolymer-based nanoplatforms	Drug delivery of paclitaxel against A549 and MCF-7 cancer cells	8
	Linear or branched oligomannose-functionalized amphiphilic Janus glycodendrimers self-assembled glycodendrimersomes	Simulation of cell membrane for probing glycan–lectin interactions	51
	Amphiphilic Janus glycopeptide dendrimers self-assembled glycopolymer nanoplatforms with diverse structures	Lectin-guided, pH-responsive drug delivery system with immunotherapeutic potential	52
	Glycopolymer nanocarriers *via* co-assembly of hydrophobic PBA-mPEG-*t*-PCL and mannoside-*b*-PCL	Mannose-guided nanocarriers for MDA-MB-231 breast cancer cell targeting with high drug payload	53
	Zwitterionic guanidiniocarbonyl pyrrole (GCP)-lactose folded glyco-nanoplatforms	Lactose-guided, pH-responsive nanocarriers for liver tumor targeting	54
	Cationic dihexadecyldimethylammonium bromide (DHDAB) and mannose-mimetic polymer co-assembled glyco-nanoplatforms	Cationic glycopolymer nanocarriers for nucleic acid delivery and cancer vaccine immunotherapy	55
	Dextran-hydroxypropyl methacrylate (HPMA) UV-triggered glyco-nanoplatforms	Photo-controlled self-assembly of dextran-stabilized nanostructures with tunable morphology	56
	Glyco-inside enzyme-responsive glyco-nanoplatforms	Controlled antigen release activated by lysosomal lipase	58
	Polymerization-induced self-assembled (PISA) glyco-nanoplatforms with internal galactose	First combination of glyco-inside strategy with reversible addition-fragmentation chain transfer (RAFT) mediate PISA for tunable glycopolymer nanoassemblies	59

Table 1 (*Contd.*)

Glyco-nanoplatform types		Applications/improved features	Ref.
	Lactose-containing glycopolymer-grafted nanosystems	Selective bacterial capture and water disinfection	60
	Glucose- or N-acetylglucosamine-based glycopolymer-grafted silica NPs	Tumor metastasis inhibition *via* anti-adhesion by glyco-nanoplatforms mimicking natural glycosaminoglycans	61
Glyco-functionalized quantum dots	Aminooxy thiol and phosphorylcholine-modified Cd-based glycodots	*In vivo* live near-infrared fluorescence imaging (NIR-FI) revealing the role of terminal sialic acids in blood circulation and biodistribution	66
	Glucose-coated CdSe/ZnS glycodots containing specific sulfonamide inhibitor	Targeted imaging of carbonic anhydrase IX-overexpressing cancer cells *via* sulfonamide inhibitor	65
	α-1,2-Manno-biose-coated CdSe/CdS glycodots	Shape-dependent multivalent lectin recognition in bacteria	68
	Glucose-coated $CuInS_2$ glycodots	Cd-free glycodots with dual visible and NIR fluorescence for biocompatible imaging	67
	Lactose-coated carbon dots	Fluorescent glyco-nanoprobes for selective lectin targeting and cellular imaging	70
	α-2,6-Sialyllactose-decorated carbon dots	Multivalent Siglec-targeting glycodots for selective binding and cytotoxicity induction in B cells	71
Glycan-based magnetic nanocomposites	Physically blended chitosan-coated magnetic nanoparticles (MNPs)	Enzyme immobilization and efficient galactooligosaccharide (GOS) production	78
	Graft-polymerized chitosan-coated MNPs	pH-responsive MNPs for high-efficiency paclitaxel delivery and cancer chemotherapy	80
	Dextran-coated superparamagnetic iron oxide (SPIO)	Magnetic resonance imaging (MRI)	82
	Cross-linked iron oxide nanoparticles (CLIO)	Diagnostic magnetic resonance, targeted MRI, positron emission tomography (PET) imaging, and photodynamic therapy	84
	Starch-coated magnetic nanocrystals	Effective purification of recombinant proteins bearing the maltose-binding motif	85
	Co-precipitated chitosan-HA magnetic nanocarriers	pH-responsive doxorubicin (DOX) nanocarriers with high encapsulation efficiency and antitumor activity against MDA-MB-231 and MCF-7 cancer cells	86
	Hydrothermally synthesized chitosan-coated MNPs	Ultrasensitive tuberculosis diagnosis *via* capturing acid-fast bacilli (AFB) from sputum Rapid *Escherichia coli* (*E. coli*) capture from leafy greens	72 and 87
	Ionically cross-linked hydrogel beads between alginate and mixed magnetic cellulose nanocrystals	Ionic hydrogel system for magnetically guided, controlled delivery of anti-inflammatory drug, ibuprofen	88
	Magnetic hydrogel nanoclusters integrated by alginate and hydrophobic MNPs	Both MRI and photoacoustic imaging	81
	Chitosan-sodium tripolyphosphate (NaTPP) ionically cross-linked magnetic nanogels	Cationic magnetic hydrogels for enhanced cancer cell uptake *via* electrostatic interaction	89
	Magnetic hydrogels stabilized by internally cross-linked HA	Tissue-regenerative hydrogels enabling cell adhesion, angiogenesis, and controlled degradation	90

Table 1 (Contd.)

Glyco-nanoplatform types	Applications/improved features	Ref.
Monosaccharide-conjugated iron oxide nanoclusters	Cell subtype differentiation by multivalent glycan–lectin recognition	91
HA-conjugated magnetic nanoplatforms integrated with indocyanine green (ICG)	Dual-modal MRI/NIR-FI for HA-mediated cancer targeting	73
Sialyl Lewis[X]-conjugated magnetic nanoparticles	Targeted imaging of inflamed endothelium by Sialyl Lewis[X]-selectin interaction	92
Glucosamine-conjugated MNPs by glutaraldehyde linkage	Selective glycoprotein concanavalin A (conA) detection and magnetic isolation through glucose–ConA interaction	93
Noncovalently glyco-coated MNPs	Magnetically guided E. coli capture and swarming modulation for biofilm research	79

commonly *via* Au–S linkages.[28] Construction of glyco-AuNPs typically relies on neoglycoconjugates bearing thiol-terminated linkers or their disulfides. These conjugates are introduced either by (1) *in situ* reduction of gold salts in the presence of thiolated glycoconjugates or (2) post ligand exchange, where thiolated glycoconjugates replace existing surface ligands on preformed nanoparticle cores. In 2001, Penadés *et al.* first described the preparation of glyco-AuNPs by the landmark Brust–Schiffrin two-phase protocol for the synthesis of thiol-derivatized AuNPs.[29] In particular, the method utilized tetraoctylammonium bromide (TOAB) as a phase transfer reagent and sodium borohydride (NaBH$_4$) as a strong reducing agent (Fig. 2a). Following the immediate addition of the capping thiolated glycoconjugates, this method provides ultra-small glyco-AuNPs with core diameters typically of 1–3 nm. By this method, different ultra-small glyco-AuNPs were achieved by employing various thiol derivatives.[30] Despite the success of this strategy, the resulting glyco-AuNPs often exhibited broad size distribution and low yield, primarily due to an increased tendency to aggregate. In addition, the use of strong reducing agents may degrade sensitive thiolated ligands, compromising the stability and functionality of glyco-AuNPs. Recently, alternative protocols have been attempted to synthesize AuNPs without relying on NaBH$_4$ as a reducing agent. Seeberger *et al.* developed a streamlined method for preparing monodisperse glucose-conjugated ultra-small AuNPs (Fig. 2b).[31] In particular, they utilized the 1-thioglucose as both a stabilizing and reducing agent, eliminating the need for an additional reducing agent. By fine-tuning the ratio of HAuCl$_4$ and 1-thio-β-D-glucose sodium, uniform glucose-AuNPs rapidly formed within seconds, though other glyco-derivatives were not involved in this method. Moreover, Jiang *et al.* reported the preparation of ultra-small AuNPs by mixing HAuCl$_4$ solution with 4,6-diamino-2-pyrimidinethiol (DAPT) in ethanol at 70 °C for 24 h.[32] Similarly, Liu *et al.* obtained AuNPs ranging from 2.4–6.1 nm by stirring a mixture of HAuCl$_4$ and thiol-ligands at 95 °C for 18 h, with particle size controlled by the ligand-to-gold ratio.[33] However, both protocols require elevated temperatures and long reaction times. To address these challenges, Polito *et al.* developed a photo-induced microfluidic strategy for the synthesis of different ultra-small glyco-AuNPs (Fig. 2c),[34] offering precise control over particle size, morphology, and reproducibility. The one-pot method enables the formation of ultra-small glyco-AuNPs at room temperature within 2 h by flowing the HAuCl$_4$ and thiol-glycoconjugates through a UV-irradiated microfluidic reactor, without extra reducing agents. Importantly, under UV light, the solvent undergoes photodecomposition, generating hydroxyl radicals and solvated electrons that serve as active reductants in the formation of ultra-small glyco-AuNPs.[34,35]

The other common strategy for constructing glyco-AuNPs with thiolated carbohydrates is post ligand exchange, where thiol-terminated glycoconjugates are introduced onto preformed AuNP cores. This approach was initially reported by Russell *et al.*,[36] who prepared mannose-stabilized AuNPs using the classical method developed by Turkevich *et al.*,[37] with sodium citrate serving as both the reducing and stabilizing agent (Fig. 3a). In this method, preheated solutions of HAuCl$_4$ and sodium citrate were rapidly mixed and stirred at 85 °C for 2.5 h. Thiolated glycans were subsequently added, and the solution was left at room temperature for 24–48 h or boiled for 1–2 min to enable partial displacement of the surface-bound citrate ions, leading to the formation of Au–S bonds and self-assembly of glyco-AuNPs.[38–41] These anisotropic glyco-AuNPs exhibit strong surface plasmon resonance (SPR) signals, enabling their applications in surface-enhanced Raman spectroscopy (SERS), biosensing, and photothermal therapy. To further enhance their SPR properties and improve carbohydrate–protein binding efficiencies, star-shaped AuNPs have been developed. Typically, they are synthesized through
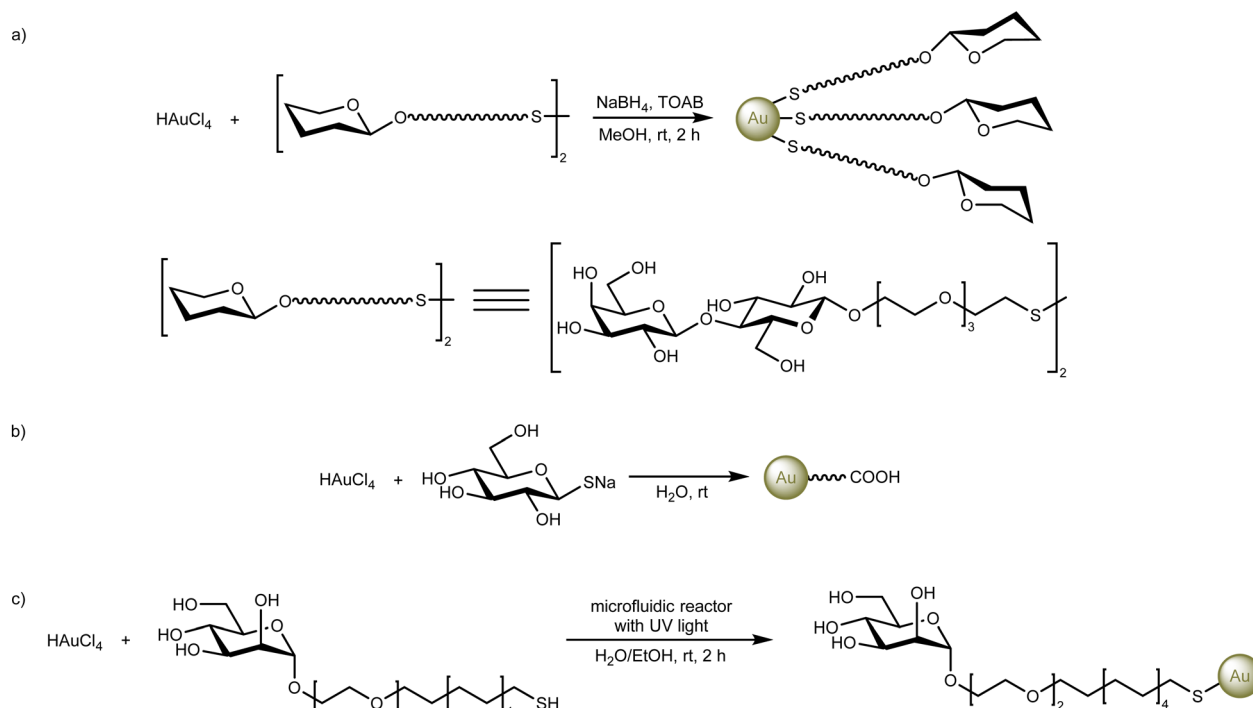
In situ reduction of gold salts in the presence of thiolated glycoconjugates

Fig. 2 Synthesis of glyco-AuNPs through *in situ* reduction of gold salts. (a) Synthesis of glyco-AuNPs by conventional $NaBH_4$ reduction; (b) synthesis of glyco-AuNPs using 1-thioglucose as both reducing and stabilizing agent; (c) photo-induced microfluidic synthesis of glyco-AuNPs.
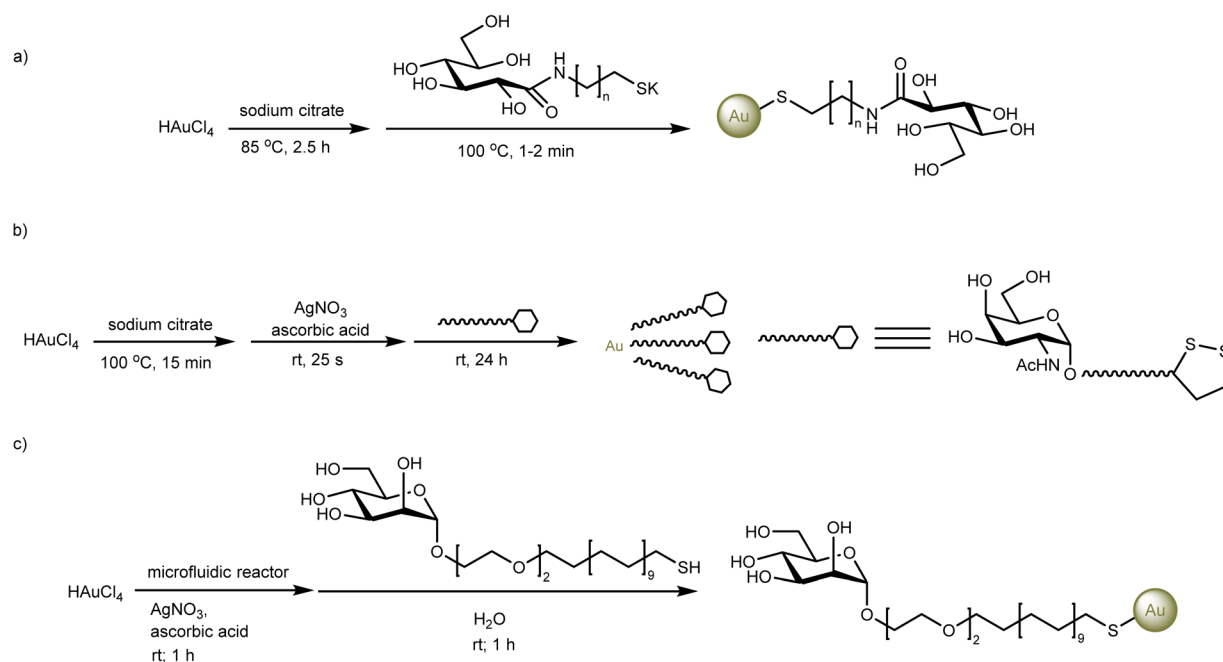
Post ligand exchange

Fig. 3 Synthesis of glyco-AuNPs through post ligand exchange. (a) Synthesis of glyco-AuNPs by conventional post ligand exchange, with sodium citrate serving as both reducing and stabilizing agent; (b) two-step synthesis of star-shaped glyco-AuNPs: seed generation using sodium citrate, followed by shape growth under ascorbic acid and sodium nitrate; (c) one-step, seedless synthesis of spherical glyco-AuNPs with high reproducibility using a microfluidic platform.

aqueous seed-mediated growth followed by shape-directed formation. For instance, Kikkeri *et al.* synthesized star-shaped glyco-AuNPs by first generating seed particles using sodium citrate as a reducing agent, followed by the addition of ascorbic acid and sodium nitrate to promote star-shaped growth.[42] Ligand exchange with various thiolated glycoconjugates was then performed to yield the final glyco-functionalized AuNPs (Fig. 3b). Notably, these star-shaped glyco-AuNPs elicited more effective immune responses compared to rod-shaped counterparts, highlighting their potential as promising platforms for vaccine development. To simplify this two-stage process, Polito *et al.* reported a one-step, seedless method conducted at room temperature under microfluidic conditions, which enables improved control over the nucleation and growth steps.[43] In this approach, ascorbic acid was employed as both the reductive and stabilizing agent, in combination with silver nitrate. Moreover, fine modulation of the silver nitrate concentration and the pH of the ascorbic acid solution allowed precise tuning of nanoplatform morphology.[44] More recently, this method was adapted by Sitia *et al.*[22] for the preparation of glyco-AuNPs. Following the formation of the spherical AuNPs, thiol-functionalized glycopolymers were introduced to generate glyco-AuNPs *via* ligand exchange (Fig. 3c). This method allows the rapid and efficient synthesis of highly reproducible glyco-AuNPs for immunotherapeutic applications.

The synthesis of glyco-AuNPs has evolved from classical methods to refined strategies, offering improved control over size, shape, and surface presentation. Ultra-small glyco-AuNPs have drawn increasing attention for their favorable pharmacokinetics, including prolonged circulation and tissue penetration.[34] Coupled with ligand exchange, glyco-NPs offer a modular platform for optimizing immune interactions and targeting specificity.[26] Looking forward, integrating microfluidic and photochemical technologies may enable scalable production of well-defined glyco-AuNPs, paving the way for their broader application in precise diagnostics and therapy.

2.2 Glycopolymer-based nanoplatforms

Glycopolymers, featuring tunable backbones and pendent glycan presentation, have been widely employed to mimic the multivalent interactions of natural glycoconjugates with lectins.[45] Their synthetic versatility allows for precise control over glycan composition, valency, and spatial arrangement,[46] making them invaluable tools in probing carbohydrate-mediated biological processes. To further enhance their performance and broaden biomedical applications, glycopolymers have been increasingly integrated into nanoplatforms, which either formed through self-assembly or by grafting glycopolymers onto nanoplatform surfaces. This provides a synergistic combination of the biological specificity of glycans and the physicochemical advantages of nanomaterials.[47] Such hybrid systems exhibit enhanced stability, prolonged circulation, improved cellular uptake, and potent multivalent binding affinities, holding the promise for applications in targeted drug delivery, vaccine development, biosensing, and antimicrobial therapies.[48,49]

Self-assembly of block copolymers represents a versatile bottom-up approach for the fabrication of functional nanomaterials, yielding well-defined nanostructures, such as micelles and vesicles, with tunable size from tens to hundreds of nanometers.[50] Various amphiphilic glycopolymers have been shown to self-organize in solution into diverse morphologies. For instance, Korzhikova-Vlakh *et al.*[8] successfully synthesized an amphiphilic poly(2-deoxy-2-methacrylamido-D-glucose)-*b*-poly(L-lysine-*co*-L-phenylalanine) (PMAG-*b*-P(Lys-*co*-Phe)) copolymer to fabricate spherical glycopolymer-based nanoplatforms (Fig. 4a). When loaded with a chemotherapy drug, paclitaxel, these nanoplatforms exhibited effective *in vitro* antitumor activity against A549 and MCF-7 cancer cells comparable to the commercial formulation paclitaxel-LANS, underscoring their potential as effective drug delivery systems. Moreover, to better mimic the structural complexity of cell-surface glycoconjugates, Percec *et al.* designed amphiphilic Janus glycodendrimers bearing sequence-defined linear or branched oligomannose units for better cellular recognition.[51] These amphiphilic glycodendrimers then self-assembled in aqueous solution into glycodendrimersomes with lamellar, raft-like membrane morphologies (Fig. 4b), facilitating multivalent glycan presentation for effective lectin binding. Additionally, Yang *et al.* developed a series of amphiphilic Janus glycopeptide dendrimers that self-assembled into structurally diverse nanostructures, such as glycospheres, worm-like micelles, and fibers, depending on the ratio of glycan to phenylalanine residues in short peptide.[52] In their design, seven saccharides were conjugated to the C-2/C-3 positions with seven di- or tetrapeptides to the C-6 position of a β-cyclodextrin core *via* dynamic acylhydrazone bonds. These dendrimers featured well-defined and tunable architectures, demonstrating strong lectin binding, pH-responsive release of hydrophobic cargos, and immunomodulatory effects, which highlights their potential for targeted drug delivery. Rather than relying solely on the self-assembly of amphiphilic glycopolymers, Lai *et al.* recently designed a co-assembly strategy in which a hydrophobic polyester, phenylboronic acid (PBA)-mPEG-*t*-poly(ε-caprolactone) (PBA-mPEG-*t*-PCL), and a mannose-functionalized block copolymer, mannoside-*b*-PCL, assembled into spherical glycopolymer-based nanoplatforms with an average diameter of 120 nm.[53] Notably, incorporation of hydrophobic PBA-mPEG-*t*-PCL enabled efficient loading of doxorubicin (DOX), reaching 20.63%, which exceeds the loading capacity reported for most NPs (0.227–20%). Leveraging both mannose-mediated tumor cell recognition and the high drug payload, the resulting glyconanoplatforms exhibited selective cytotoxicity toward MDA-MB-231 breast cancer cells.

Beyond traditional amphiphilic self-assembly, alternative unique strategies have been designed to construct glycopolymer-based nanoplatforms. For instance, Giese *et al.* synthesized a lactose-functionalized glycopolymer incorporating guanidiniocarbonyl pyrrole (GCP) zwitterionic units, where reversible and pH-responsive supramolecular cross-linking drove the folding of single polymer chains into small nanoplatforms (<40 nm) in aqueous solution.[54] This approach not only enabled the assembly of nanoplatform from single
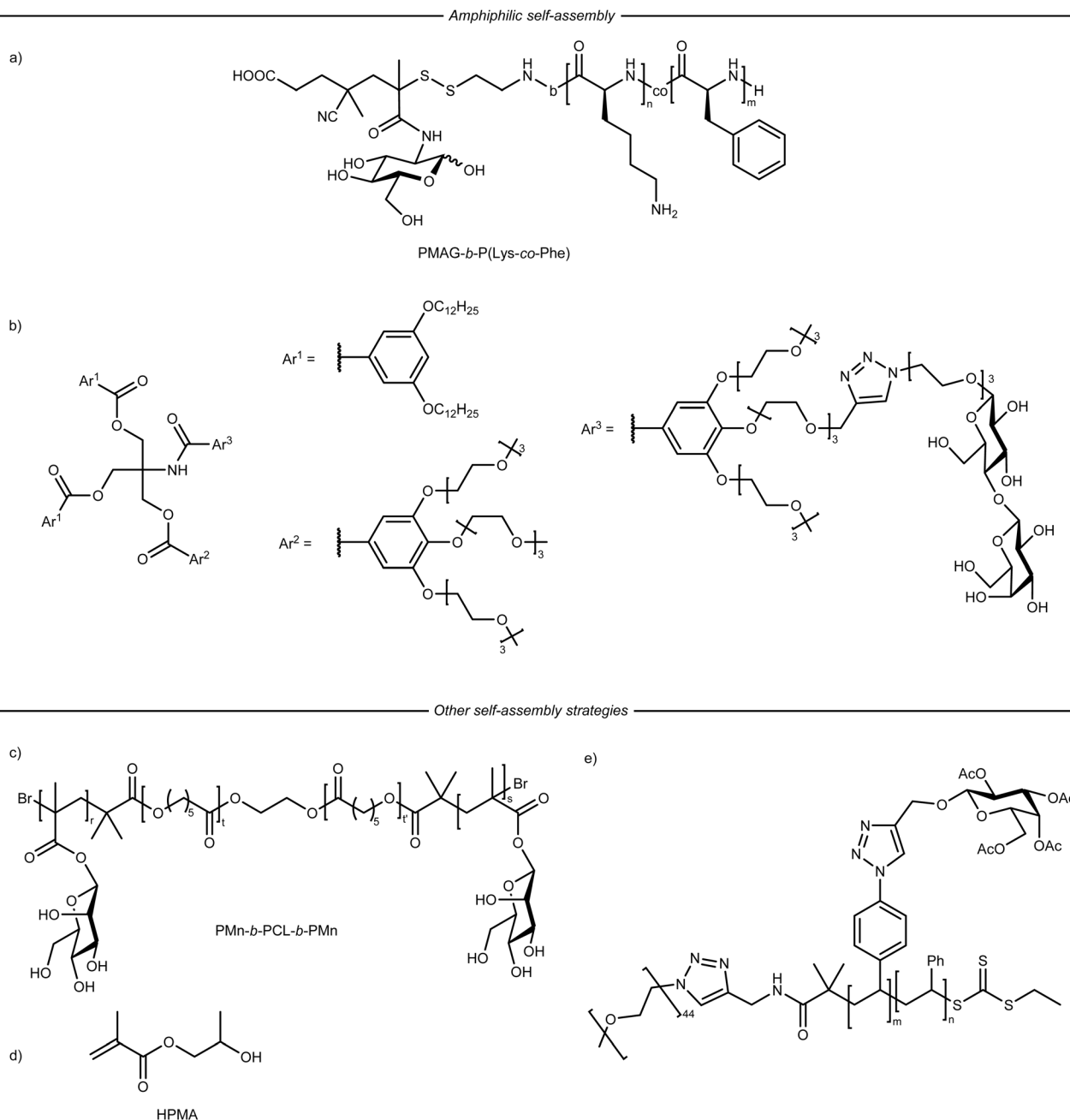
Fig. 4 Representative glycopolymer structures employed in the formation of glycopolymer-based nanoplatforms *via* self-assembly. (a) Structure of amphiphilic PMAG-*b*-P(Lys-*co*-Phe) copolymer forming spherical glycopolymer-based nanoplatforms; (b) structure of amphiphilic Janus glycodendrimers bearing sequence-defined oligomannose for the formation of glycodendrimersomes; (c) structure of mannose-mimicking ABA-type triblock copolymer (PMn-*b*-PCL-*b*-PMn), which electrostatically co-assembles with dihexadecyldimethylammonium bromide (DHDAB); (d) structure of hydroxypropyl methacrylate (HPMA) grafted onto dextran backbone, enabling UV-induced self-assembly into nanostructures; (e) representative glycopolymer structure applied in the "glyco-side" strategy.

polymers but also provided a sharp and switchable pH-response mechanism for controlled drug release that is distinct from conventional acid-labile linker cleavage. Owing to the presence of lactose moieties, the resulting glycopolymer-based nanoplatforms exhibited potential for targeted delivery to HepG2 liver cancer cells. Separately, Chakravarty *et al.* constructed glycopolymeric nanoplatforms by co-assembling a mannose-mimicking ABA-type triblock copolymer (PMn-*b*-PCL-*b*-PMn) with the cationic surfactant dihexadecyldimethylammonium

bromide (DHDAB) (Fig. 4c).[55] The electrostatically driven co-assembly resulted in stable, well-defined positively charged nanoplatforms capable of encapsulating nucleic acids, which not only protected nucleic acids from enzymatic degradation but also promoted dendritic cell uptake and activation through electrostatic interactions with negatively charged membranes, supporting their potential as vaccine carriers for cancer immunotherapy. In addition to attaching sugar monomers onto different polymers, Six *et al.* first utilized the reversible addition-

fragmentation chain transfer (RAFT) method to graft water-soluble monomer hydroxypropyl methacrylate (HPMA) onto a dextran backbone, a widely used neutral and biodegradable polysaccharide (Fig. 4d).[56] By controlling the UV-irradiation "on" or "off", the HPMA segments underwent self-assembly to eventually form polymer-based nanoplatforms with diverse well-defined structures, ranging from spherical micelles to worm-like micelles and vesicles. Instead of acting as a terminal or branched ligand, dextran served as a water-soluble steric stabilizer in this strategy.[57]

Due to the synthetic complexity, low efficiency, and structural heterogeneity often associated with direct conjugation of free glycans onto polymer backbones,[58] alternative strategies have been explored to achieve multivalent glycan presentation. One such approach is the "glyco-inside" design, in which protected glycan units are embedded within the hydrophobic core of amphiphilic polymers. Upon deprotection, these internal glycans become exposed, enabling controlled structural transformation and immunological activation. Jiang et al. implemented the "glyco-inside" strategy, in which sugar moieties were internally embedded within amphiphilic block copolymers rather than presented terminally (Fig. 4e).[58] Upon enzymatic deprotection by lysosomal lipase, the polymers underwent a distinct morphology transition from vesicles to micelles, accompanied by the release of encapsulated antigens. This work represents the first report of enzyme-triggered deprotection-induced self-assembly of glycopolymers. Importantly, the responsiveness to endogenous lysosomal lipase eliminates the need for external triggers, offering a biologically relevant platform for immunoactive glyco-nanostructures. Moreover, Xing et al. first combined the "glyco-inside" strategy with RAFT-mediated polymerization-induced self-assembly (PISA) to construct glycopolymer nanoassemblies with tunable morphologies.[59] The galactose-bearing monomer, 6-O-methacryloyl-1,2 : 3,4-di-O-isopropylidene-D-galactopyranose (MAIGP), underwent in situ self-assembly using poly((2-dimethylamine)ethyl methacrylate) as the chain transfer agent. By increasing the lengths of PMAIGP, the resulting glyco-nanoplatforms exhibited distinct morphologies, including branched worms, highly branched worms, multilayer lamellae, and complex vesicles. This work highlights the potential of integrating "glyco-inside" design with PISA for the scalable and controlled fabrication of structurally defined glyco-nanomaterials.

In addition to self-assembly approaches, grafting glycopolymers onto nanoplatform surfaces has emerged as a robust strategy to construct glyco-nanostructures with defined surface functionality and enhanced biointerface control. For instance, Zhang et al. synthesized lactose-containing glycopolymers via Cu(0)-mediated polymerization and grafted them onto $Fe_3O_4@TiO_2$ nanoplatforms (Fig. 5a).[60] The glycopolymer shell improved the dispersibility of nanoplatforms and enabled selective adhesion to Escherichia coli (E. coli) through carbohydrate–lectin recognition. The resulting hybrids maintained the photocatalytic antibacterial activity of TiO_2 under UV irradiation and allowed for facile magnetic recovery. This study offers an efficient approach for constructing glyco-functionalized

photocatalysts with enhanced stability and bacterial capture capability for water disinfection applications. Furthermore, Chen et al. developed glycopolymer-grafted silica nanostructures by RAFT polymerization of glucose- or N-acetylglucosamine-derived monomers (Fig. 5b).[61] Notably, the uniform spherical glyco-nanoplatforms exhibited significant multivalent effects, leading to effective inhibition of tumor metastasis by disrupting tumor cell-platelet adhesion and cell interaction. This work offers a structurally defined and cost-effective approach for mimicking natural glycosaminoglycans with promising biomedical potential.

These studies demonstrate the expanding utility of glycopolymer-based nanoplatforms, which offer tunable nanostructures, multivalent engagement, and enhanced biointerface control. Critically, the choice of polymer design and fabrication strategy significantly influences NP's performance in targeting, stability, and therapeutic delivery. Despite these advances, several challenges persist, including the synthetic complexity of glycopolymer, difficulty in precise spatial control of glycan distribution, and limited understanding of long-term in vivo pharmacokinetics and distribution.[62,63] Therefore, integrating advanced polymerization techniques with nanoscale engineering will facilitate the creation of programmable glyco-nanoplatforms for further biomedical applications.

2.3 Glyco-functionalized quantum dots

Quantum dots (QDs) have garnered increasing attention as versatile nanomaterials for multicolor imaging, diagnostics, and targeted drug delivery both in vitro and in vivo, owing to their broad absorption spectra, high fluorescence efficiency, and prolonged photostability.[64] When functionalized with glycan moieties, glycodots integrate the superior optical advantages of QDs with the water solubility, biocompatibility, and selective recognition capabilities of glycans.[65,66] These hybrid nanomaterials have emerged as promising platforms for bioimaging, biosensing, and therapeutic applications, driving the development of glycodots bearing diverse glycan types.[65–67] This section classifies glycodots based on their core composition, with a focus on recent advances in metal- and carbon-based glycodots.

Most metal-based glycodots are primarily composed of cadmium-based metal cores with ZnS or ZnSe as protective shells. Functionalization with carbohydrate ligands improves their circulation time and enables targeted recognition of specific biomolecules. For example, Nishimura and co-workers prepared a library of Cd-based glycodots, CdSe/ZnS and CdSeTe/CdS, by coating QDs with a simple mixture of two monothiol ligands, phosphorylcholine and aminooxy-thiol. In this design, phosphorylcholine provided good water solubility, remarkable stability across pH ranges, long-term durability, and preserved fluorescence brightness, offering a superior alternative to conventional PEG-based ligands. Meanwhile, aminooxy-thiol enabled efficient oxime ligation with ketone-functionalized sugars, such as α-sialic acid, α-glucose, and α-mannose. This platform later enabled live animal near-infrared fluorescence imaging (NIR-FI), uncovering for the first time the necessity of
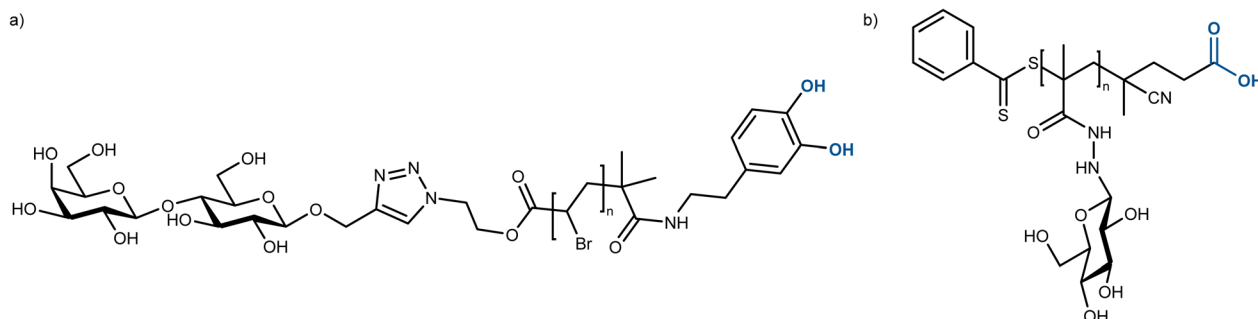
Grafting glycopolymers onto NPs

Fig. 5 Representative glycopolymer structures for the formation of glycopolymer-based nanoplatforms by grafting glycopolymers onto nanosystems. (a) Structure of lactose-containing glycopolymers grafted onto core nanoplatforms; (b) structure of glucose-derived glycopolymers grafted onto silica nanoplatforms. Conjugating moieties are highlighted in blue.

terminal sialic acid residues in extending the circulation time and biodistribution of glycodots *in vivo*.[66] Building on the similar concept of a mixed-ligand surface, Richichi *et al.* designed a multifunctional glycodot platform based on CdSe/ZnS QDs using a dual-ligand coating (Fig. 6a).[65] A glucose-attached ligand served as a stabilizing agent to prevent aggregation in biological fluids, while the other, containing a specific sulfonamide inhibitor, conferred active targeting of the cancer biomarker carbonic anhydrase IX (CA IX). The resulting glycodots demonstrated selective binding of bladder cancer cells overexpressing CA IX, with no binding observed in control cells lacking the protein. This work highlights the unique integration of colloidal stability and specific molecular recognition with the superior optical properties of QDs, yielding a robust nanoprobe for targeted cancer imaging. Advancing beyond the dual-ligand,

spherical QD design, Guo *et al.* recently introduced a structurally refined glycodot by employing elongated CdSe/CdS QDs coated with a single ligand presenting α-1,2-manno-biose (DiMan) to investigate how glycodot's shape affects multivalent lectin–glycan interactions.[68] Using two structurally similar tetrameric lectins, DC-SIGN and DC-SIGNR as models, they demonstrated that scaffold curvature dictates distinct binding modes. This work highlights glycodots as mechanistic probes for shape-selective lectin recognition and guides the rational design of glyco-nanoplatforms for targeting multivalent lectins. Despite their promising optical properties, Cd-based QDs pose significant cytotoxicity risks due to the release of heavy metal Cd^{2+} ions under physiological conditions, which limits their biomedical applicability. This concern has prompted growing interest in developing Cd-free glycodots with reduced toxicity.
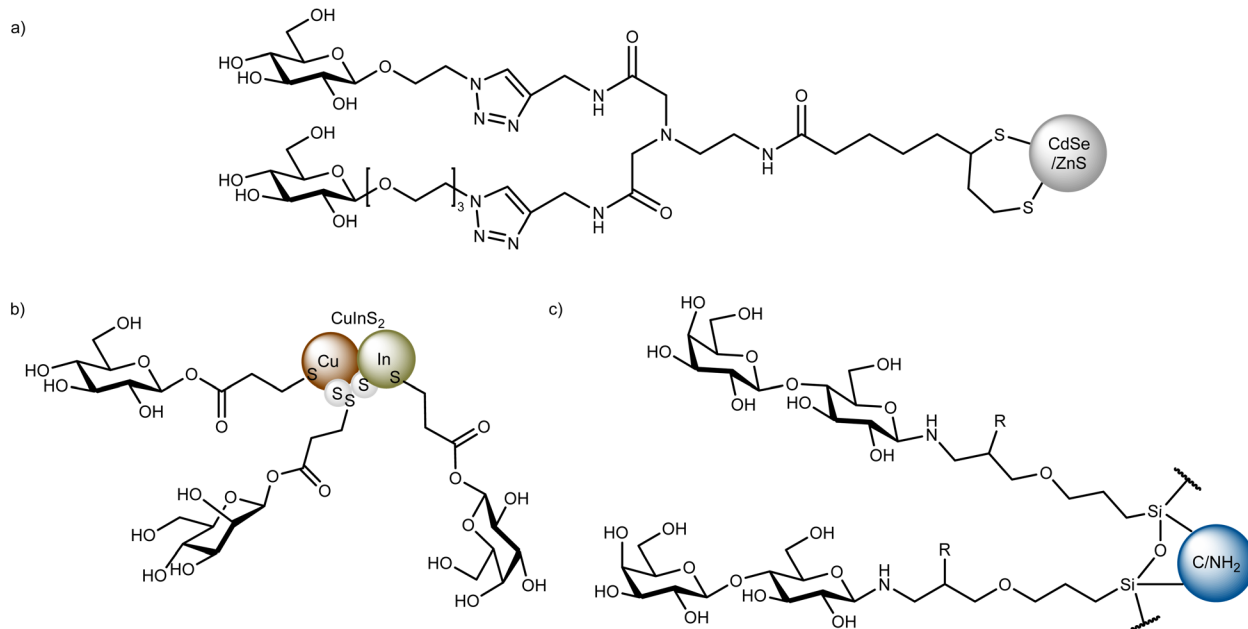
Different types of glycodots

Fig. 6 Representative structures of different types of glycodots. (a) Structure of a glycodot based on conventional CdSe/ZnS quantum dots (QDs) coating with glucose-derived ligand; (b) structure of glyco-CuInS$_2$ QDs free of heavy metals; (c) structure of lactose-derived carbon dots (CDs).

Among alternatives, copper indium sulfide ($CuInS_2$) QDs, free of heavy metals, have emerged as a biocompatible candidate, offering tunable photoluminescence, broad absorption, and good stability. Lei's group developed water-soluble glyco-$CuInS_2$ QDs with monodisperse (Fig. 6b).[67] They exhibited distinct dual fluorescence: visible and NIR fluorescence, attributed to excitonic and surface defect emissions, respectively.

Carbon dots (CDs) are the emerging alternatives to the toxic and expensive metal-based semiconductor QDs and organic dyes for biomedical applications.[69] The CDs are less than 10 nm in size and possess distinct tunable optical properties. Size controlling, heteroatom doping, and surface functionalization are the most promising synthesis methods for developing tunable CDs. For instance, Tiralongo et al. developed a simple and efficient approach to prepare lactose-functionalized CDs (Fig. 6c).[70] CDs were synthesized via thermal treatment of citric acid and polyethylenimine (PEI), followed by lactose modification using a self-assembled glycan monolayer (SAGM) strategy. These lactose-coated CDs exhibited strong binding affinities to lectins, selective cellular uptake, and efficient intracellular localization, demonstrating their potential as fluorescent bioimaging nanoprobes. Following a similar method, Tiralongo and co-workers subsequently reported the synthesis of a new class of multivalent sialic acid-binding immunoglobulin-like lectin (Siglec) probes by decorating fluorescent CDs with α-2,6-sialyllactose ligands. Enhanced glycan density on the CD surface altered binding preference, allowing α-2,6-sialyllactose ligands to bind Siglec-1. Importantly, α-2,6-sialyllactose-CDs exhibited micromolar affinity (approximately 70 μM of IC_{50}) for Siglec-2 (CD22) and induced cytotoxicity in CD22-overexpressing B cells, attributed to glycan clustering on the CD surface.[71] These glycodots act as high-affinity molecular tools for probing Siglec and hold promise for targeted cancer immunotherapy.

Glycodots represent a versatile nanoplatform that combines the superior optical properties of QDs with the specific recognition capabilities of glycans. Although Cd-based glycodots have advanced our understanding of multivalent interactions, such as curvature-dependent lectin binding, their clinical application remains limited due to toxicity concerns. Recent advances in metal-free glycodots, $CuInS_2$- and carbon-based glycodots, provide safer, tunable alternatives with comparable optical performance. The controlled display of multivalent glycans on these nanostructures has enabled novel strategies for immune modulation and cancer targeting, underscoring the expanding potential of glycodots as next-generation tools in biomedical research.

2.4 Glycan-based magnetic nanocomposites

For decades, magnetic nanocomposites, typically composed of iron oxides, have attracted substantial interest for biomedical applications owing to their desirable features, such as tunable magnetic responses to external fields and utility as contrast agents in magnetic resonance imaging (MRI).[72,73] Harnessing these attributes, they have been extensively explored for cancer treatments, tissue engineering, and bioseparation.[74–76]

However, bare magnetic nanocomposites often face limitations in vivo. Specifically, they tend to aggregate due to magnetic dipole–dipole interactions, lose magnetism upon oxidation, and are rapidly cleared by phagocytes, causing poor biodistribution and shortened circulation.[77] Surface functionalization with natural glycans offers a practical strategy to address these challenges.[78,79] Polysaccharides such as starch, chitosan, cellulose, dextran, and hyaluronic acid (HA), as well as simple sugars like glucose, mannose, and galactose, not only stabilize magnetic cores and improve biocompatibility but also introduce functional interfaces for further biological interactions. These glycan coatings support targeted drug delivery,[80] enzyme immobilization,[78] and multimodal imaging.[81] Through such modifications, basic magnetic nanocomposites can be upgraded into versatile, biofunctional platforms.

The most straightforward approach to preparing glyco-based magnetic nanocomposites is the blending method, which involves the physical incorporation of pre-synthesized magnetic nanocomposites into a polysaccharide solution. For instance, Abdin et al.[78] developed chitosan-functionalized magnetic nanoparticles (MNPs) by blending Fe_3O_4 MNPs with chitosan in acetic acid for enzyme immobilization and large-scale galactooligosaccharide (GOS) production (Fig. 7a). Chitosan served as both a stabilizing shell and a functional interface for covalent attachment of β-glucosidase from Thermotoga maritima (T. maritima). This glycan layer enhanced colloidal stability, while the magnetic core allowed for rapid recovery and reuse through external magnetic guidance. The immobilized system retained over 40% enzymatic activity after six cycles and outperformed the free enzyme in GOS yield, highlighting the synergistic advantages of glycan-based surface engineering and magnetic nanotechnology for developing recyclable and high-performance biocatalytic platforms. To further enhance delivery efficiency, Anirudhan et al.[80] advanced the conventional blending approach by integrating graft polymerization. In their design, the blending method was employed merely as an initial step to coat magnetic iron oxide NPs with chitosan, creating a biocompatible interface. The core innovation lay in the subsequent in situ free radical polymerization of [2-(methacryloyloxy)ethyl] trimethyl ammonium chloride (METAC) and ethylene glycol dimethacrylate (EGDMA) onto the chitosan-coated MNPs, forming a robust, cross-linked polymeric network. This modification significantly enhanced the encapsulation efficiency of hydrophobic antitumor drug, paclitaxel, to 96.7%, and enabled pH-responsive, controlled drug release. The resulting nanocarrier demonstrated excellent anticancer efficacy, hemocompatibility, and pharmacokinetic properties.

Although the blending method is simple and cost-effective, its reliance on weak physical interactions often leads to poor dispersion and MNP leakage. To overcome these limitations, several methods have been developed. Among them, in situ co-precipitation directly mixes iron oxide with a polysaccharide matrix to allow MNPs to nucleate and grow in situ, ensuring uniform distribution, stronger interfacial interactions, and enhanced structural stability. A well-established example of the co-precipitation strategy is the synthesis of dextran-coated iron oxide NPs. MacKenzie et al.[82] first reported the preparation of
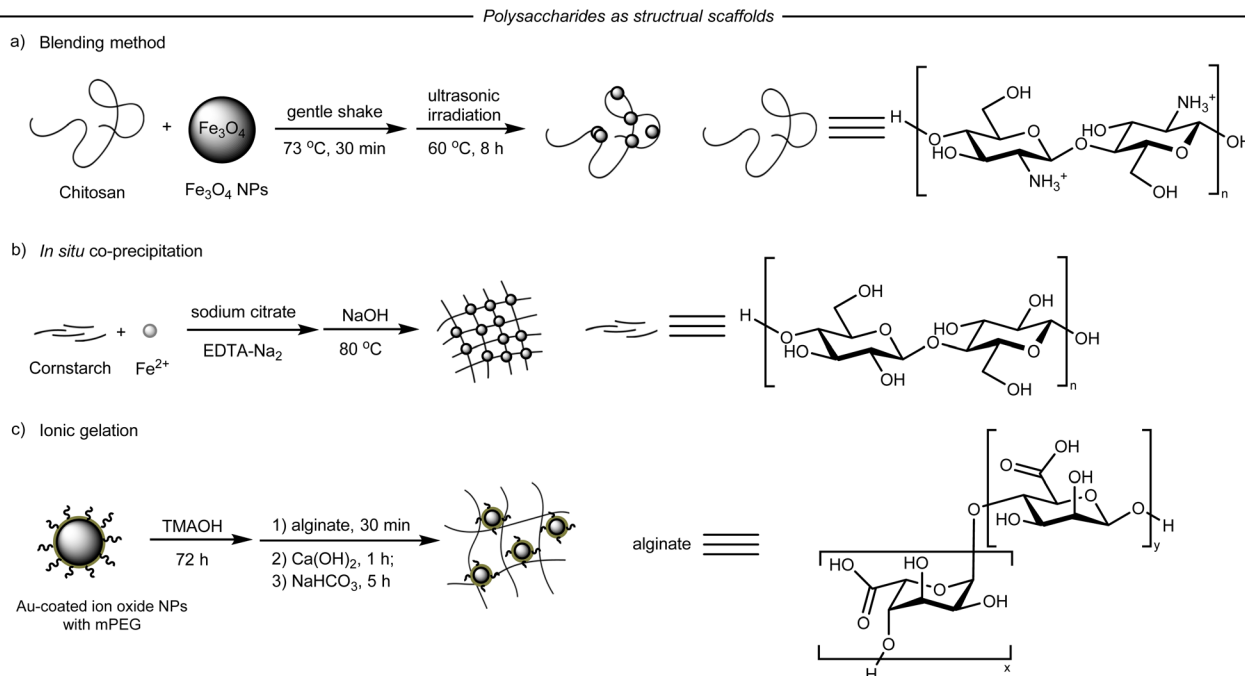
Fig. 7 Representative glyco-based magnetic nanocomposites in which polysaccharides act as structural scaffolds. (a) Synthesis of chitosan-based magnetic nanosystems by the blending method; (b) synthesis of starch-based magnetic nanocrystals with uniform particle distribution by *in situ* co-precipitation; (c) synthesis of glyco-based magnetic hydrogels with negatively charged alginate by ionic gelation.

30–40 nm dextran-coated superparamagnetic iron oxide (SPIO) by co-precipitating iron salts in an alkaline solution with dextran. Subsequent periodate oxidation and reductive amination enabled conjugation of *Staphylococcus aureus* (*S. aureus*) protein A, facilitating efficient immunolabelling and magnetic separation of antibody-tagged cells using simple permanent magnets. The dextran-coated SPIO has been proved by the U.S. FDA as an MRI contrast agent, especially for hepatic imaging. However, their rapid clearance by the liver and spleen limits their utility for targeted applications. To address this, Weissleder and co-workers[83] developed monocrystalline iron-oxide NPs (MION), yielding 4–5 nm single-crystal cores with reproducible colloidal and magnetic properties for target specific MRI. Nevertheless, the noncovalent association between the iron core and dextran shell rendered the structure susceptible to dissociation under physiological conditions. Therefore, the MIONs were further modified by cross-linking the dextran shell with epichlorohydrin (cross-linked iron oxide nanoparticles, CLIO), followed by surface animation to finally give CLIO-NH$_2$.[84] This cross-linked formulation significantly improved *in vivo* stability and introduced abundant reactive amine groups, enabling efficient conjugation of targeting ligands and fluorophores for robust and multimodal imaging applications. Moreover, the co-precipitation strategy has been extended to a variety of polysaccharide systems. For instance, Frank *et al.*[85] employed a co-precipitation method to prepare starch-coated magnetic iron oxide nanocrystals with an average size of 11.5 nm and a narrow distribution (Fig. 7b). In this system, starch functioned not only as a stabilizer but also as a template, promoting uniform particle distribution and enabling effective affinity purification of several recombinant proteins bearing the maltose-binding motif. While this system remained confined to sorbent applications, Rezaei *et al.*[86] adapted the co-precipitation strategy within a blended chitosan-HA matrix, followed by κ-carrageenan cross-linking, to construct multifunctional magnetic nanocarriers. This design achieved a high encapsulation efficiency of 83% and enabled pH-responsive release of DOX, with up to 84% release at pH 5.5, demonstrating potent antitumor activity against both MDA-MB-231 and MCF-7 cancer cells. Moreover, the hydrothermal method has also been employed to facilitate *in situ* magnetite nucleation under controlled high-temperature and high-pressure conditions, simultaneously enabling glycan coupling to form well-defined and stable nanostructures with uniform dispersion and reduced leakage. A notable example is the development of chitosan-based MNPs for capturing acid-fast bacilli (AFB) from sputum, as demonstrated by Alocilja *et al.*[72] In this system, ferric chloride and sodium acetate were dissolved in ethylene glycol and heated in a sealed Teflon-lined vessel at 200 °C for 15 h, with chitosan added directly during synthesis, to generate the final MNPs with a glycan shell of 10–50 nm. When used in combination with Tween 80 as a dispersant, the glycan-based MNPs improved AFB quantification by up to 445% compared with smear microscopy, offering a rapid, low-cost, and sensitive diagnostic tool for tuberculosis. A similar nanocomposite was later applied to pathogen detection in food matrices by the same group,[87] which enabled the rapid capture of *E. coli* directly from leafy greens within 60 min, as confirmed by transmission electron microscopy.

A milder and widely adopted technique for synthesizing glycan-based magnetic hydrogels is ionic gelation, which relies on the electrostatic interactions between ionic cross-linking agents and

glycans while encapsulating MNPs. Within such hydrogels, polysaccharides typically serve as stabilizers, enhancing structural integrity and regulating drug release. For instance, Bushra et al.[88] developed magnetic hydrogel beads for model drug delivery by the ionic gelation method. They first mixed magnetic cellulose nanocrystals (m-CNCs), an alginate matrix, and an anti-inflammatory drug, ibuprofen. Upon the addition of CaCl$_2$, the ionic cross-linking was induced between the negatively charged carboxylate group on alginate and Ca^{2+}, yielding magnetic hydrogel beads capable of ibuprofen delivery. To address the incorporation of hydrophobic MNPs into hydrogels, Seo et al.[81] employed a phase-transfer agent, tetramethylammonium hydroxide (TMAOH), which allowed stable dispersion of hydrophobic MNPs within alginate (Fig. 7c). Subsequent cross-linking with Ca^{2+} generated hydrogel nanoclusters suitable for dual-mode MRI and photoacoustic imaging, overcoming the challenge of stabilizing hydrophobic nanoplatforms in biological systems. More recently, Dureja et al.[89] introduced a strategic material shift by utilizing chitosan, a positively charged polymer, in combination with sodium tripolyphosphate (NaTPP) as the ionic linker. The gelation occurred via electrostatic interactions between the chitosan amine groups and the phosphate groups of the NaTPP. The recruitment of chitosan possesses the MNPs with a positive charge surface, facilitating uptake by cancer cells, which tend to have a negatively charged surface. Furthermore, to extend the stabilizer role of the glycan matrix, HA was first incorporated into magnetic hydrogels owing to its unique roles in tissue regeneration, wound healing, and drug delivery, as reported by Liu et al.[90] HA, as essential polysaccharide found in natural tissues like skin and cartilage, was covalently cross-linked with trace peptide impurities retained from the extraction process via 1-ethyl-3-(3-dimethylaminopropyl)carbodiimide/N-hydroxysuccinimide (EDC/NHS) chemistry to form HA-MNP hydrogels. In this system, HA not only stabilized the hydrogel network but also enabled controlled degradation, supported cell adhesion, and promoted angiogenesis, highlighting their promise for tissue regeneration.

Apart from structural polysaccharides, certain glycans have been post-conjugated onto magnetic nanocomposites to serve as specific targeting ligands via glycan–lectin interactions. Among the available conjugation strategies, amide bond formation remains the most commonly employed method for anchoring glycans onto the surface of magnetic composites. For example, Huang et al.[91] conjugated various monosaccharides, including mannose, galactose, fucose, and sialic acid, onto iron oxide NPs via amide bonds formed between sugar carboxyl groups and surface amines (Fig. 8a). Additionally, alkyne-modified N-acetylglucosamine was attached through click chemistry to azide-functionalized MNPs. The resulting clusters of glyco-conjugated MNPs demonstrated the ability to differentiate not only cancer cells from normal cells, but also closely related and metastatic cancer cell subtypes. In their subsequent study,[73] HA-conjugated MNPs were prepared through a similar amide bond linkage between HA and aminated MNPs, the latter obtained via co-precipitation with dextran and subsequent amination with ammonium hydroxide. Notably, this work marked the first application of HA in MNPs for cancer-targeting imaging through specific HA–lectin interaction. Moreover,

incorporation of indocyanine green (ICG) endowed the system with dual-modal capability, enabling both MRI and NIR-FI for enhanced diagnostic accuracy and sensitivity. In another example, Harms et al.[92] recruited EDC/NHS coupling strategy to form amide bonds by reacting NHS-activated MNPs with amino-functionalized oligosaccharide, Sialyl Lewis^X (SX) (Fig. 8b), a well-established ligand of E- and P-selectin, to yield SX@MNPs. These selectin proteins are expressed on vessel endothelium during inflammation, where they mediate leukocyte recruitment to sites of injury. Importantly, exploiting the SX-selectin interaction, these nanocomposites bound selectively to inflamed endothelium with enhanced multivalent affinity and accumulated in brain vasculature after experimental stroke in vivo, highlighting promise for noninvasive detection of endothelial activation. In addition to amide bond conjugation, Basiruddin et al.[93] recently utilized glutaraldehyde-based coupling (Fig. 8c). In this approach, the dialdehyde glutaraldehyde acts as a linker between the amine groups of glucosamine and pre-synthesized MNP surface, forming imine bonds that were subsequently reduced and stabilized by NaBH$_4$. The glucose-functionalized MNPs demonstrated specific and selective binding to the glycoprotein concanavalin A (ConA), which has a known affinity for glucose. Upon binding, the magnetic nanocomposites aggregated and were readily separated magnetically, allowing efficient protein detection and isolation. Whereas the previous studies relied on covalent conjugation of glycans to MNP surfaces, alternative non-covalent approaches have also been investigated. Silva et al.[79] reported MNPs coated with carbohydrates like glucose, galactose, sucrose, and maltose via chemical adsorption, achieved by mixing with uncoated MNPs and stirred at 70 °C for 20 min (Fig. 8d). While the glycan layers contributed to stabilization and biocompatibility, their key role was in mediating bacterial binding. Binding assays revealed glycan-dependent bacterial association, with glucose- and galactose-coated MNPs preferentially binding E. coli and enabling efficient magnetization. Notably, glucose-coated MNPs also modulated E. coli swarming formation under a magnetic field, highlighting their potential as low-cost, biocompatible tools to manipulate bacterial communities for biofilm studies and drug evaluation. These diverse approaches offer versatile strategies for conjugating glycans onto MNP surfaces, facilitating the construction of biofunctional magnetic nanoplatforms with specific targeting capabilities.

3 Glyco-nanoplatforms toward mammalian cells

Due to their specific recognition by lectins on cancer and immune cell surfaces, glycans have been widely employed as targeting ligands in delivery systems to direct therapeutic agents to specific cell types or stimulate host immune responses. This glycan-mediated targeting strategy has demonstrated broad utility in glycan-based cancer therapy, biosensing, and immunomodulation.[94–98] Several representative carbohydrate–lectin pathways have been extensively explored for biomedical applications.
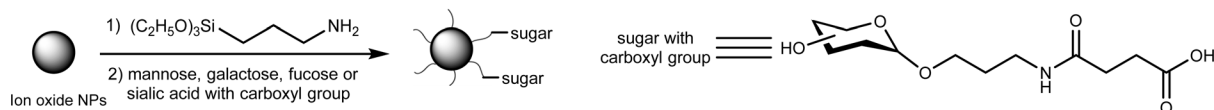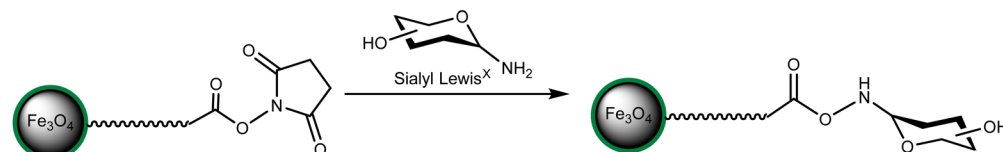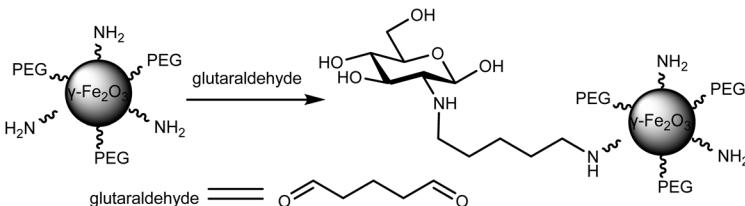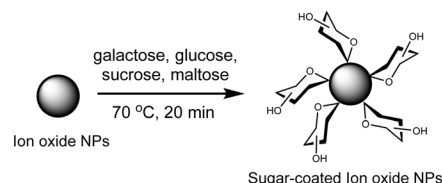
Fig. 8 Representative glyco-based magnetic nanocomposites with carbohydrates serving as targeting ligands. (a) Synthesis of glyco-grafted magnetic nanoparticles (MNPs) by amide bond formation between carboxylated glycans and aminated MNPs; (b) synthesis of Sialyl Lewis^X-grafted MNPs by EDC/NHS coupling strategy; (c) synthesis of glucose-functionalized MNPs using a glutaraldehyde linker; (d) synthesis of sugar-coated MNPs by chemical adsorption.

In cancer cells, three major glycan–lectin interacting pathways have been widely utilized. First, the glucose transporter (GLUT) family, comprising various isoforms expressed on the cell surface, is frequently overexpressed in a wide range of tumors.[99,100] These transporters recognize different saccharides, such as glucose, mannose, and fructose (Fig. 9a), facilitating efficient cellular uptake of glycan-conjugated nanosystems and enhancing therapeutic efficacy. Second, the asialoglycoprotein receptor (ASGPR), a liver-specific transmembrane protein upregulated in hepatocellular carcinoma (HCC) cells, selectively binds galactose/lactose and N-acetylgalactosamine via its Ca^{2+}-dependent carbohydrate recognition domain (Fig. 9b), enabling ligand internalization through ASGPR-mediated endocytosis.[101–103] Third, CD44, a cell-surface glycoprotein overexpressed in various tumor cells, plays a critical role in cell adhesion and migration.[104,105] Its high binding affinity for HA has led to the widespread use of HA-functionalized nanoplatforms in tumor imaging and drug delivery (Fig. 9c).[106,107]

Among immune cells, one of the most important lectins is the mannose or galactose receptor, known as CD206, which is highly expressed on tumor-associated macrophages (TAMs) (Fig. 9d), within the tumor microenvironment (TEM).[108] Targeting CD206 has been recognized as a promising strategy to reprogram TEM. The nanoplatforms bearing CD206-binding glycans have been shown to induce the repolarization of anti-inflammatory M2 macrophages into pro-inflammatory M1 phenotypes,[109,110] thereby converting the "cold" tumors into "hot" ones and enhancing antitumor efficiency.

3.1 Glycan-directed cancer therapy

The selective recognition between glycans and overexpressed lectin receptors on cancer cells has been increasingly harnessed to enhance the specificity and efficacy of anticancer therapies. For instance, Pei et al. decorated a nanoprodrug system with lactose to achieve ASGPR-mediated targeting, enabling selective cytotoxicity toward HepG2 hepatocellular carcinoma cells while markedly minimizing off-target effects on HL7702 normal liver cells.[111] Building on this targeting strategy, our group developed a theranostic galactose-modified AuNPs conjugated with a fluorophore and prodrug. The system leveraged galactose-ASGPR interactions, achieving preferential accumulation in HepG2 cells over HeLa and HEK293T cells, confirming ASGPR-dependent cellular selectivity.[103] Recently, Lai et al. synthesized a mannose-functionalized nanoplatform, which was efficiently internalized by MDA-MB-231 breast cancer cells via mannose receptors, resulting in a significant suppression of tumor cell proliferation.[53]

3.2 Glycan-based biosensing

Leveraging the specific interactions between carbohydrates and receptors overexpressed on cancer and immune cell surfaces, glyco-decorated nanoplatforms have long served as targeting ligands for biosensing applications. Previously, our group developed a novel noncovalent "turn-off/turn-on" biosensor system using fluorescein boronic acid and mannose-modified AuNPs. In this design, fluorescence signal was initially quenched upon interaction with the glyco-AuNPs but restored by the addition of carbohydrate-specific lectin, enabling sensitive biosensing.
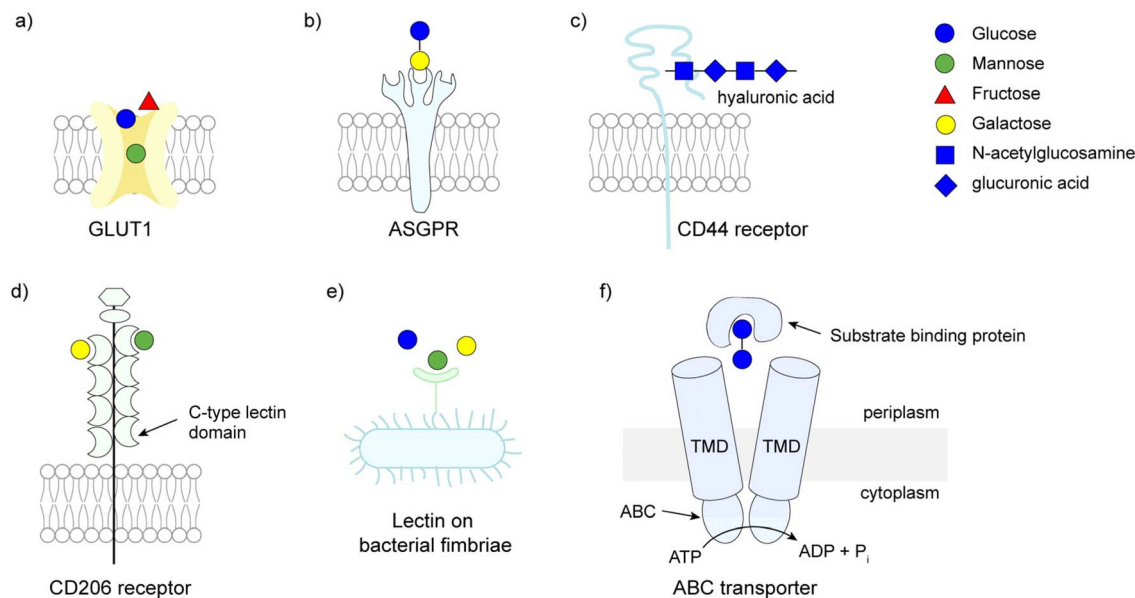
Fig. 9 Summary of carbohydrate–lectin interactions in mammalian cells (a–d) and bacterial cells (e and f). (a) Glucose, mannose, and fructose can be recognized and transported by GLUT1; (b) liver specific transmembrane protein, ASGPR, specially binds lactose; (c) CD44, overexpressed in tumor cell surface, binds hyaluronic acid; (d) CD206 in M2 macrophages serves as the mannose or galactose receptor; (e) mannose, glucose, and galactose selectively binds to the lectins on bacterial fimbriae; (f) ATP-dependent ABC transporter on cell membrane enables the transport of maltose into the cytoplasm. TMD: transmembrane domain.

Interestingly, intracellular uptake was observed in Jurkat human T lymphoma cells, highlighting the dual potential of this non-covalent platform for both biosensing and drug delivery.[12] Rather than relying on additional fluorescence, Huang *et al.* recently reported the real-time SERS imaging of breast cancer tissue through the HA-conjugated AuNPs.[41] The installation of the HA ligand significantly enhanced the tumor-targeting efficiency through its specific binding to CD44 receptors. Although the optimized SERS-NPs enabled stable and high-resolution biosensing in tumor tissues, their ability to penetrate dense tumor regions was limited. To address this, Lei *et al.*[67] developed glyco-CuInS$_2$ QDs by conjugating different monosaccharides, including galactose, glucose, and mannose, onto the QD surface. *In vitro* imaging revealed excellent membrane-targeting properties of glycodots in HeLa, A549, and MKN-45 cancer cells. Remarkably, their highly negative zeta potential enabled deep penetration into the interior of 3D tumor spheroids. Beyond solid tumors, effective nanocarrier delivery across physiological barriers such as the blood–brain barrier (BBB) remains a major obstacle. Hrubý *et al.* developed glucose-conjugated solid lipid nanoparticles (SLNs) to enhance BBB permeability *via* GLUT1-mediated transport. *In vitro* studies using hCMEC/D3 cells confirmed significantly improved intracellular uptake of glucosylated SLNs compared to unmodified controls,[112] underscoring the potential of glucose conjugation for brain-directed drug delivery.

3.3 Glycan-driven immunomodulation

Immunotherapy has emerged as a powerful clinical strategy for treating infectious diseases and cancer.[113–116] Yeh *et al.* identified CD206 as an effective target for cancer immunotherapy.[117] By decorating with β-D-galactopyranoside, the glyco-AuNPs selectively targeted CD206-expressing TAMs in lung cancer. These glyco-AuNPs exhibited enhanced tumor accumulation and, when combined with anti-PD-1 treatment, significantly boosted T cell activation and suppressed tumor growth. To minimize systemic immune activation induced by glycan–lectin engagement, Sitia *et al.* recently developed mannose-functionalized AuNPs (Man-AuNPs) that selectively target liver macrophages.[22] In a colorectal cancer liver metastasis model, Man-AuNPs reprogrammed tumor-associated macrophages toward a pro-inflammatory phenotype by upregulating related cytokines. Moreover, to enhance cancer immunotherapy by activating dendritic cells (DCs), Hu and co-workers[118] first conjugated the DC-targeting ligand, mannose, directly to a model antigen, ovalbumin (OVA), creating a mannose–antigen conjugate (MAN-OVA). In this system, mannose engagement of C-type lectins on DCs promoted receptor-mediated uptake and directed OVA into the MHC class I processing pathway, leading to the subsequent activation of tumor-killing CD8$^+$ T cells. Conversely, in a primary biliary cholangitis model, they suppressed inflammatory cytokine expression while promoting anti-inflammatory responses. These dual, context-dependent immunomodulatory effects are likely mediated by mannose-induced metabolic modulation. Man-AuNPs exhibited strong liver tropism and minimal systemic toxicity, offering a promising strategy for localized immunomodulation in both cancer and autoimmune diseases.

Glycan-mediated targeting offers a versatile platform across cancer therapy, biosensing, and immunomodulation. By leveraging the specific interactions between glycans and lectins on cancer and immune cells, glycan-functionalized nano-carriers can improve delivery specificity, enhance diagnostic accuracy, and enable immune reprogramming. These diverse

applications highlight the broad potential of glycan–lectin interactions in advancing targeted biomedical strategies.

4 Glyco-nanoplatforms toward bacterial cells

Fimbriae on the bacterial surface are decorated with various lectins that enable specific binding to sugars such as mannose, galactose, and fucose (Fig. 9e).[119–121] These glycan–lectin interactions have been exploited for bacterial targeting in both diagnostic and antimicrobial applications. Additionally, ATP-binding cassette (ABC) transporters located on the bacterial membrane have been leveraged to capture maltose- or maltodextrin-functionalized nanosystems for antibacterial treatments (Fig. 9f).[23,122]

4.1 Glycan-driven bacterial infection inhibition

Glycan–lectin interactions offer a powerful strategy for selectively targeting drug-resistant pathogenic bacteria. For instance, our group designed galactose-functionalized black phosphorus nanosheets to co-deliver the antibiotic kanamycin and enable photothermal therapy against *Pseudomonas aeruginosa* PAO1 (*P. aeruginosa* PAO1), a Gram-negative, drug-resistant strain.[121] In this system, bacterial capture was mediated through galactose-specific recognition. *In vivo* mouse studies confirmed that the glyco-nanosheets achieved comparable antibacterial activities. Following a similar binding mode, Zhang and co-workers[123] developed an acid-responsive polymeric glyco-nanoplatform to eradicate the drug-resistant *P. aeruginosa* and disrupt its protective biofilm. The dual-targeting NPs were synthesized by self-assembling two acid-degradable block copolymers, functionalized with galactose ligands for LecA lectin binding and guanidine moieties for electrostatic bacterial capture. The photosensitizer Chlorin e6 (Ce6) was encapsulated within the core and released in response to the acidic biofilm microenvironment. Upon 660 nm light irradiation, reactive oxygen species were generated, achieving 95% bacterial killing and >70% biofilm disruption, while minimizing off-target toxicity. Moreover, the ATP-driven ABC transporter was exploited by Yan *et al.* to enhance pathogen localization during bacterial infection inhibition.[23] They engineered D-maltose-capped gold nanoclusters (AuNC-Mal), leveraging the specific recognition of D-maltose by ABC transporters on *P. aeruginosa* PAO1. Upon activation with thiourea (TU), antimicrobial species such as $[Au(TU)_2]^+$ and smaller AuNCs were generated, achieving a minimum inhibitory concentration of 1 μg mL^{-1} and exhibiting 30–60-fold lower *in vitro* cytotoxicity toward mammalian cells.

4.2 Glycan-based bacterial detection

Beyond bacterial eradication, surface lectin interactions have also been harnessed for the detection of drug-resistant bacteria. For instance, Kumar *et al.* reported the synthesis of silver NPs (AgNPs)-loaded gel microspheres functionalized with glucose, mannose, or galactose for simultaneous bacterial detection and inhibition.[13] The glycan moieties enabled selective binding to bacterial cell walls, while AgNPs formed *in situ* imparted potent antimicrobial activity. Among them, mannose-functionalized

microspheres exhibited the fastest bacterial capture kinetics and effective inhibition against *E. coli* and antibiotic-resistant *S. aureus*. Bacterial detection was visually indicated by microsphere aggregation and a characteristic color change of AgNPs, providing a versatile platform for rapid bacterial sensing. Moreover, the dual-mode mannose-based biosensor was synthesized by Zhou *et al.*[124] to simultaneously identify mannose-binding bacterial species and quantify their adhesion strength. The sensor featured a gold electrode modified with AuNPs and a self-assembled mannose monolayer, enabling selective capture of bacteria expressing mannose-binding lectins. Leveraging SERS, the platform generated molecular fingerprints, which were analyzed *via* partial least squares discriminant analysis (PLS-DA) for accurate species differentiation. Meanwhile, electrochemical impedance spectroscopy (EIS) quantified binding affinities of the nano-biosensor, revealing significantly stronger adhesion of *Salmonella typhimurium* (*S. typhimurium*) compared to *E. coli* JM109. This integrated strategy overcomes the specificity limitations of conventional glycan sensors, offering both qualitative and quantitative insights from a single device. In addition to aggregation-based and SERS detection strategies, Nazari *et al.*[125] recently developed a label-free electrochemical biosensor for the rapid, sensitive, and selective detection of *E. coli*. Constructed on a glassy carbon electrode modified with AuNPs, the sensor featured a covalently attached mannose derivative, *p*-carboxyphenylamino mannose (PCAM), which specifically binds the FimH adhesin on *E. coli* type I fimbriae. Upon bacterial binding, the electron transfer to the electrode is impeded, resulting in an increase resistance measured by EIS. The sensor achieved an ultralow detection limit of 2 CFU mL^{-1} with a broad dynamic range (1.3×10^1 to 1.3×10^6 CFU mL^{-1}) and delivered results within 60 min. With excellent selectivity and performance in real samples such as tap water and milk, this cost-effective platform offers a practical tool for on-site microbial monitoring.

These advances underscore the potential of glyco-nanoplatforms to improve both diagnostic accuracy and therapeutic efficacy in combating antimicrobial resistance. Moving forward, a deeper mechanistic understanding of glycan-lectin interactions may drive the development of programmable nanosystems capable of strain-specific targeting, real-time detection, and potent antimicrobial activity.

5 Summary and outlook

In this perspective, we focused on the recent advances in the preparation of different types of glyco-nanoplatforms and discussed their potential biomedical application in both mammalian cells and drug-resistant bacteria. Leveraging a wide range of synthetic strategies, glyco-AuNPs, glycopolymer-based nanoplatforms, glycodots, and glycan-based magnetic nanocomposites have been developed with distinct structural features, enabling enhanced binding affinities, stability, biodistribution, and delivery efficiency. By mimicking naturally multivalent glycan displays, glyco-nanoplatforms have emerged as versatile platforms that harness the specificity of glycan–

lectin interactions for targeted therapy, diagnostics, and immunomodulation.

While glyco-nanoplatforms have shown great promise in preclinical studies, their clinical translation remains challenging.[16,17] The next frontier lies in moving beyond proof-of-concept systems toward clinically viable therapeutics and diagnostics. Achieving this goal requires addressing several critical barriers. First, the synthetic complexity and scalability of glycan conjugation pose major limitations, particularly for structurally defined glycans and multivalent architectures.[7] To address these limitations, the field is increasingly adopting chemoenzymatic[126,127] and automated synthetic routes[128] to generate well-defined glycan moieties. These are coupled with modular anchoring scaffolds, such as lipids, polymers, or peptides, functionalized with orthogonal click handles to facilitate efficient and site-specific conjugation.[91,129] Emerging technologies like continuous-flow or microfluidic systems offer improved batch-to-batch reproducibility, while integrated analytical tools, such as glycan-release mass spectrometry[130,131] and lectin-array profiling,[132] are becoming standard for in-process quality control. Together, these technological advances will pave the way for scalable, reproducible, and clinically translatable glyco-nanoplatforms.

Second, a deeper understanding of how glycan density, spatial arrangement, and morphology of nanoplatforms influence *in vivo* behavior is essential. In complex clinical environments, rapid formation of the protein corona can obscure surface-displayed glycans, hinder glycan–lectin interactions, and alter biodistribution. Strategic optimization of nanoplatform architecture and surface composition may help mitigate these effects and preserve targeting specificity.[133] Instead of attempting to eliminate coronas, glyco-based nanoplatforms should bias their composition and evolution toward beneficial, tissue-specific soft coronas while avoiding hard, masking layers. This goal can be advanced by tuning polymer chemistry and presentation to regulate which proteins are recruited. For instance, glycosylated polyhydroxy scaffolds with optimized amino to hydroxyl ratios suppress immunoglobulin adsorption in circulation while preferentially recruiting tumor-associated proteins like CD44 or osteopontin within the tumor interstitium, thereby extending circulation and enhancing selective uptake.[133] Additionally, utilizing patchy or textured interfaces may reduce overall protein adsorption relative to smooth surfaces and help prevent corona-driven disruption of glycan–lectin targeting.[134] Finally, explicit consideration of glycans within the corona is needed. Corona glycosylation modulates uptake and immune signaling, and deglycosylated coronas increase macrophage adhesion, uptake, and pro-inflammatory cytokines.[135] Therefore, the designed glyco-based nanosystem should preserve favorable glycan shielding while minimizing unintended glycans.

Third, the heterogeneity of lectin expression in patient populations and disease states further demands the development of personalized or programmable glyco-nanoplatforms capable of adaptive targeting and response. To support this, tissue-mapping techniques such as spatial glycan profiling,[136] lectin staining,[132,137] or single-cell receptor sequencing[138,139] can be utilized to uncover clinically targetable microenvironments like Siglec-high myeloid subsets, thereby allowing for more precise patient selection. Building on these maps, programming systems can be built using interchangeable glycan libraries on a shared scaffold to rapidly align ligand motifs with disease-specific phenotypes. Mixed-glycan presentations and microenvironment-responsive coatings that respond to local tissues further reduce off-target accumulation. As detailed in Sections 3 and 4, our group has developed programmable and multifunctional systems for both therapeutic and diagnostic applications. We are now extending our work to tackle highly heterogeneous, treatment-resistant indications, including tumors resistant to immune checkpoint inhibitors (ICIs) and severe infections caused by methicillin-resistant *S. aureus* and carbapenem-resistant *P. aeruginosa,* through designing modular nanoplatforms with tunable glycan ligands and unique killing strategies. With continued advances in glycan engineering and nanofabrication, glyco-nanoplatforms hold the promise to become next-generation platforms for targeted therapy, biosensing, and immunomodulation in clinical settings, paving the way to unlock the therapeutic power of the glyco-code.

Author contributions

Conceptualization: X.-W. L., X.-L. Z., and H. D.; original draft: X.-W. L. and X.-L. Z.; review and editing: all authors; funding acquisition: X.-W. L. and H. C.; project administration: X.-W. L.; supervision: X.-W. L.

Conflicts of interest

The authors declare no conflicts of interest.

Data availability

No primary research results, software, or code have been included, and no new data were generated or analysed as part of this perspective.

Acknowledgements

Notes and references

1 K. El-Boubbou and X. Huang, *Curr. Med. Chem.*, 2011, **18**, 2060.

2 S. Wisnovsky and C. R. Bertozzi, *Curr. Opin. Struct. Biol.*, 2022, **75**, 102395.

3 K. Arora, P. M. Sherilraj, K. A. Abutwaibe, B. Dhruw and S. L. Mudavath, *Int. J. Biol. Macromol.*, 2024, **268**, 131511.

4 M. Marradi, F. Chiodo, I. García and S. Penadés, *Chem. Soc. Rev.*, 2013, **42**, 4728.

5 J. Ramos-Soriano, M. Ghirardello and M. C. Galan, *Chem. Soc. Rev.*, 2022, **51**, 9960.

6 C. Pritchard, M. Ligorio, G. D. Jackson, M. I. Gibson and M. D. Ward, *ACS Appl. Mater. Interfaces*, 2023, **15**, 36052.

7 L. Su, Y. Feng, K. Wei, X. Xu, R. Liu and G. Chen, *Chem. Rev.*, 2021, **121**, 10950.

8 N. Zashikhina, M. Levit, A. Dobrodumov, S. Gladnev, A. Lavrentieva, T. Tennikova and E. Korzhikova-Vlakh, *Polymers*, 2022, **14**, 1677.

9 H. Khan, H. R. Mirzaei, A. Amiri, E. K. Akkol, S. M. A. Halimi and H. Mirzaei, *Semin. Cancer Biol.*, 2021, **69**, 24.

10 J. J. Barchi Jr, *Front. Immunol.*, 2022, **13**, 852147.

11 T. Mosaiab, D. C. Farr, M. J. Kiefel and T. A. Houston, *Adv. Drug Deliv. Rev.*, 2019, **151**, 94.

12 B. K. Gorityala, Z. Lu, M. L. Leow, J. Ma and X.-W. Liu, *J. Am. Chem. Soc.*, 2012, **134**, 15229.

13 J. K. Ajish, P. N. Rao, S. Bhakta, S. Kota and K. S. A. Kumar, *Colloids Surf., A*, 2024, **696**, 134305.

14 A. Ahmad, P. G. Georgiou, A. Pancaro, M. Hasan, I. Nelissen and M. I. Gibson, *Nanoscale*, 2022, **14**, 13261.

15 T. Kopac, *Int. J. Biol. Macromol.*, 2021, **169**, 290.

16 A. D. Dessai, A. Nair, N. Selvasudha, S. Garg and U. Y. Nayak, *Int. J. Biol. Macromol.*, 2025, 147830.

17 S. Đorđević, M. M. Gonzalez, I. Conejos-Sánchez, B. Carreira, S. Pozzi, R. C. Acúrcio, R. Satchi-Fainaro, H. F. Florindo and M. A.-O. Vicent, *Drug Delivery Transl. Res.*, 2022, **12**, 500.

18 P. Singh, S. Pandit, V. R. S. S. Mokkapati, A. Garg, V. Ravikumar and I. Mijakovic, *Int. J. Mol. Sci.*, 2018, **19**, 1979.

19 M.-C. Daniel and D. Astruc, *Chem. Rev.*, 2004, **104**, 293.

20 Y. Xia, Y. Xiong, B. Lim and S. E. Skrabalak, *Angew. Chem., Int. Ed.*, 2009, **48**, 60.

21 R. M. Ferrando, L. Lay and L. Polito, *Drug Discov. Today Technol.*, 2020, **38**, 57.

22 J. F. Alarcon, P. P. Schmidt, N. Panini, F. Caruso, M. B. Violatto, N. G. Sukubo, A. Martinez-Serra, C. B. Ekalle-Soppo, A. Morelli, G. Y. Moscatiello, C. Grasselli, A. Corbelli, F. Fiordaliso, J. Kelk, L. Petrosilli, G. D'Orazio, R. M. Ferrando, A. V. Ferrer, C. Fornaguera, L. Lay, S. Fumagalli, S. Recchia, M. P. Monopoli, L. Polito, P. Bigini and G. Sitia, *Adv. Sci.*, 2025, **12**, 2407458.

23 W. Ndugire, D. Truong, N. G. H. Raviranga, J. Lao, O. Ramström and M. Yan, *Angew. Chem., Int. Ed.*, 2023, **62**, e202214086.

24 R. Zhang, F. Kiessling, T. Lammers and R. M. Pallares, *Drug Delivery Transl. Res.*, 2023, **13**, 378.

25 S. Sangabathuni, R. V. Murthy, P. M. Chaudhary, M. Surve, A. Banerjee and R. Kikkeri, *Nanoscale*, 2016, **8**, 12729.

26 X. Ning, D. Budhadev, S. Pollastri, I. Nehlmeier, A. Kempf, I. Manfield, W. B. Turnbull, S. Pöhlmann, A. Bernardi, X. Li, Y. Guo and D. Zhou, *JACS Au*, 2024, **4**, 3295.

27 B. Kang, T. Opatz, K. Landfester and F. R. Wurm, *Chem. Soc. Rev.*, 2015, **44**, 8301.

28 W. A. A. Rosero, A. B. Barbezan, C. D. de Souza and M. E. C. M. Rostelato, *Pharmaceutics*, 2024, **16**, 255.

29 J. M. de la Fuente, A. G. Barrientos, T. C. Rojas, J. Rojo, J. Cañada, A. Fernández and S. Penadés, *Angew. Chem., Int. Ed.*, 2001, **40**, 2257.

30 H. Shinchi, F. Komaki, M. Yuki, H. Ohara, N. Hayakawa, M. Wakao, H. B. Cottam, T. Hayashi, D. A. Carson, T. Moroishi and Y. Suda, *ACS Chem. Biol.*, 2022, **17**, 957.

31 S. Varela-Aramburu, C. Ghosh, F. Goerdeler, P. Priegue, O. Moscovitz and P. H. Seeberger, *ACS Appl. Mater. Interfaces*, 2020, **12**, 43380.

32 Y. Xie, J. Yang, J. Zhang, W. Zheng and X. Jiang, *Angew. Chem., Int. Ed.*, 2020, **59**, 23471.

33 Y. Tan, K. He, B. Tang, H. Chen, Z. Zhao, C. Zhang, L. Lin and J. Liu, *ACS Nano*, 2020, **14**, 13975.

34 P. P. Schmidt, K. Pagano, C. Lenardi, M. Penconi, R. M. Ferrando, C. Evangelisti, L. Lay, L. Ragona, M. Marelli and L. Polito, *Angew. Chem., Int. Ed.*, 2023, **62**, e202210140.

35 E. di Marzo, R. M. Ferrando, L. Polito, L. Ragona, K. Pagano, G. D'Orazio and L. Lay, *Carbohydr. Res.*, 2025, **553**, 109508.

36 D. C. Hone, A. H. Haines and D. A. Russell, *Langmuir*, 2003, **19**, 7141.

37 J. Turkevich, P. C. Stevenson and J. Hillier, *Discuss. Faraday Soc.*, 1951, **11**, 55.

38 S. Zhang, Y. Hang, J. Wu, Z. Tang, X. Li, S. Zhang, L. Wang, J. L. Brash and H. Chen, *ACS Appl. Mater. Interfaces*, 2020, **12**, 22066.

39 C. K. Adokoh, F. K. Keter, H. H. Kinfe, R. Tshikhudo and J. Darkwa, *RSC Med. Chem.*, 2020, **11**, 283.

40 A. N. Baker, S.-J. Richards, S. Pandey, C. S. Guy, A. Ahmad, M. Hasan, C. I. Biggs, P. G. Georgiou, A. J. Zwetsloot, A. Straube, S. Dedola, R. A. Field, N. R. Anderson, M. Walker, D. Grammatopoulos and M. I. Gibson, *ACS Sens.*, 2021, **6**, 3696.

41 K. Liu, A. K. M. A. Ullah, A. Juhong, C.-W. Yang, C.-Y. Yao, X. Li, H. L. Bumpers, Z. Qiu and X. Huang, *Small Sci.*, 2024, **4**, 2300154.

42 S. Toraskar, P. M. Chaudhary and R. Kikkeri, *ACS Chem. Biol.*, 2022, **17**, 1122.

43 A. Silvestri, L. Lay, R. Psaro, L. Polito and C. Evangelisti, *Chem.–Eur. J.*, 2017, **23**, 9732.

44 M. Marelli, F. Bossola, G. Spinetti, E. Sangalli, V. D. Santo, R. Psaro and L. Polito, *ACS Appl. Mater. Interfaces*, 2020, **12**, 38522.

45 C. L. A. Nutting, J. Lefley, Z. Varanaraja, G. Yilmaz and C. R. Becer, *Polym. Chem.*, 2024, **15**, 5023.

46 J. Wang, J. Zhou, Y. Ding, X. Hu and Y. Chen, *Polym. Chem.*, 2023, **14**, 2414.

47 M. R. Thalji, A. A. Ibrahim, K. F. Chong, A. V. Soldatov and G. A. M. Ali, *Top. Curr. Chem.*, 2022, **380**, 45.

48 G. Yilmaz and C. R. Becer, *Polym. Chem.*, 2015, **6**, 5503.

49 P.-D. Ly, K.-N. Ly, H.-L. Phan, H. H. T. Nguyen, V.-A. Duong and H. V. Nguyen, *Frontal Nanotechnol. Res.*, 2024, **6**, 1456939.

50 H. Cabral, K. Miyata, K. Osada and K. Kataoka, *Chem. Rev.*, 2018, **118**, 6844.

51 Q. Xiao, M. Delbianco, S. E. Sherman, A. M. R. Perez, P. Bharate, A. Pardo-Vargas, C. Rodriguez-Emmenegger, N. Y. Kostina, K. Rahimi, D. Söder, M. Möller, M. L. Klein, P. H. Seeberger and V. Percec, *Proc. Natl. Acad. Sci. U. S. A.*, 2020, **117**, 11931.

52 F. Bi, J. Zhang, Z. Wei, D. Yu, S. Zheng, J. Wang, H. Li, Z. Hua, H. Zhang and G. Yang, *Biomacromolecules*, 2022, **23**, 128.

53 Y.-H. Huang, G. Sivakumar, R. Kamaraj, K. Y. Lim, Y.-X. Chen, C.-H. Liu, Y.-C. Wang, H.-Y. Chen, T. W. Wong, Y. W. Hau and C.-H. Lai, *Drug Delivery Transl. Res.*, 2025, **15**, 3936.

54 S. Saha, M. Klein-Hitpaß, C. Vallet, S. K. Knauer, C. Schmuck, J. Voskuhl and M. Giese, *Biomacromolecules*, 2020, **21**, 2356.

55 K. Bhamidipati, N. M. R. Nakka, M. Ahmed, K. Javvaji, R. Banerjee, N. Puvvada, A. V. S. Sainath and S. Chakravarty, *Bioorg. Chem.*, 2024, **152**, 107711.

56 K. Ferji, P. Venturini, F. Cleymand, C. Chassenieux and J.-L. Six, *Polym. Chem.*, 2018, **9**, 2868.

57 D. Ikkene, A. A. Arteni, H. Song, H. Laroui, J. L. Six and K. Ferji, *Carbohydr. Polym.*, 2020, **234**, 115943.

58 W. Qi, Y. Zhang, J. Wang, G. Tao, L. Wu, Z. Kochovski, H. Gao, G. Chen and M. Jiang, *J. Am. Chem. Soc.*, 2018, **140**, 8851.

59 L. Qiu, H. Zhang, T. Bick, J. Martin, P. Wendler, A. Böker, U. Glebe and C. Xing, *Angew. Chem., Int. Ed.*, 2021, **60**, 11098.

60 B. Wang, C. Shang, Z. Miao, S. Guo and Q. Zhang, *Eur. Polym. J.*, 2021, **142**, 110159.

61 J. Gu, Y. Li, G. Lu, Y. Ma, Y. Zhang and J. Chen, *Int. J. Biol. Macromol.*, 2023, **253**, 126975.

62 M. H. Stenzel, *Macromolecules*, 2022, **55**, 4867.

63 M. Martínez-Bailén, J. Rojo and J. Ramos-Soriano, *Chem. Soc. Rev.*, 2023, **52**, 536.

64 Y. Wang, L. Peng, J. Schreier, Y. Bi, A. Black, A. Malla, S. Goossens and G. Konstantatos, *Nat. Photonics*, 2024, **18**, 236.

65 G. Biagiotti, A. Angeli, A. Giacomini, G. Toniolo, L. Landini, G. Salerno, L. D. C. Mannelli, C. Ghelardini, T. Mello, S. Mussi, C. Ravelli, M. Marelli, S. Cicchi, E. Menna, R. Ronca, C. T. Supuran and B. Richichi, *ACS Appl. Nano Mater.*, 2021, **4**, 14153.

66 T. Ohyanagi, N. Nagahori, K. Shimawaki, H. Hinou, T. Yamashita, A. Sasaki, T. Jin, T. Iwanaga, M. Kinjo and S.-I. Nishimura, *J. Am. Chem. Soc.*, 2011, **133**, 12507.

67 X. Guan, L. Zhang, S. Lai, J. Zhang, J. Wei, K. Wang, W. Zhang, C. Li, J. Tong and Z. Lei, *J. Nanobiotechnol.*, 2023, **21**, 118.

68 J. Hooper, D. Budhadev, D. L. F. Ainaga, N. Hondow, D. Zhou and Y. Guo, *ACS Appl. Nano Mater.*, 2023, **6**, 4201.

69 J. Liu, R. Li and B. Yang, *ACS Cent. Sci.*, 2020, **6**, 2179.

70 O. Cooper, E. Eftekhari, J. Carter, B. Mallard, J. Kaur, M. J. Kiefel, T. Haselhorst, Q. Li and J. Tiralongo, *ACS Appl. Nano Mater.*, 2020, **3**, 7804.

71 O. Cooper, M. Waespy, D. Chen, S. Kelm, Q. Li, T. Haselhorst and J. Tiralongo, *Nanoscale Adv.*, 2022, **4**, 5355.

72 C. Gordillo-Marroquín, H. J. Sánchez-Pérez, A. Gómez-Velasco, M. Martín, K. Guillén-Navarro, J. Vázquez-Marcelín, A. Gómez-Bustamante, L. Jonapá-Gómez and E. C. Alocilja, *Biosensors*, 2022, **12**, 29.

73 C.-W. Yang, K. Liu, C.-Y. Yao, B. Li, A. Juhong, A. K. M. A. Ullah, H. Bumpers, Z. Qiu and X. Huang, *ACS Appl. Mater. Interfaces*, 2024, **16**, 27055.

74 G. Paltanea, V. Manescu, I. Antoniac, A. Antoniac, I. V. Nemoianu, A. Robu and H. Dura, *Int. J. Mol. Sci.*, 2023, **24**, 4312.

75 E. Aram, M. Moeni, R. Abedizadeh, D. Sabour, H. Sadeghi-Abandansari, J. Gardy and A. Hassanpour, *Nanomaterials*, 2022, **192**, 206.

76 I. J. Bruce and T. Sen, *Langmuir*, 2005, **21**, 7029.

77 J. Nowak-Jary and B. Machnicka, *J. Nanobiotechnol.*, 2022, **20**, 305.

78 F. Alnadari, Y. Xue, A. Almakas, A. Mohedein, A. Samie, M. Abdel-Shafi and M. Abdin, *J. Food Biochem.*, 2021, **45**, e13589.

79 L. A. A. Neto, T. M. Pereira and L. P. Silva, *Mater. Sci. Eng., C*, 2020, **116**, 111267.

80 V. Manjusha, M. R. Rajeev and T. S. Anirudhan, *Int. J. Biol. Macromol.*, 2023, **235**, 123900.

81 J. C. Park, D. H. Kim, T. Y. Park, H. J. Cha and J. H. Seo, *Biomacromolecules*, 2019, **20**, 4150.

82 R. S. Molday and D. Mackenzie, *J. Immunol. Methods*, 1982, **52**, 353.

83 T. Shen, R. Weissleder, M. Papisov, A. Bogdanov Jr. and T. J. Brady, *Magn. Reson. Med.*, 1993, **29**, 599.

84 C. Tassa, S. Y. Shaw and R. Weissleder, *Acc. Chem. Res.*, 2011, **44**, 842.

85 V. V. Krasitskaya, A. N. Kudryavtsev, R. N. Yaroslavtsev, D. A. Velikanov, O. A. Bayukov, Y. V. Gerasimova, S. V. Stolyar and L. A. Frank, *Int. J. Mol. Sci.*, 2022, **23**, 5410.

86 M. A. Anbardan, S. Alipour, G. R. Mahdavinia and P. F. Rezaei, *Int. J. Biol. Macromol.*, 2023, **253**, 126805.

87 S. A. Sharief, O. Caliskan-Aydogan and E. Alocilja, *Biosens. Bioelectron.:X*, 2023, **13**, 100322.

88 J. Supramaniam, R. Adnan, N. H. Mohd Kaus and R. Bushra, *Int. J. Biol. Macromol.*, 2018, **118**, 640.

89 M. Dahiya, R. Awasthi, J. P. Yadav, S. Sharma, K. Dua and H. Dureja, *Int. J. Biol. Macromol.*, 2023, **242**, 124919.

90 R. Daya, C. Xu, N.-Y. T. Nguyen and H. H. Liu, *ACS Appl. Mater. Interfaces*, 2022, **14**, 11051.

91 K. El-Boubbou, D. C. Zhu, C. Vasileiou, B. Borhan, D. Prosperi, W. Li and X. Huang, *J. Am. Chem. Soc.*, 2010, **132**, 4490.

92 T. D. Farr, C.-H. Lai, D. Grünstein, G. Orts-Gil, C.-C. Wang, P. Boehm-Sturm, P. H. Seeberger and C. Harms, *Nano Lett.*, 2014, **14**, 2130.

93 S. K. Basiruddin, *J. Sci. Res.*, 2024, **16**, 331.

94 B. K. Gorityala, J. Ma, X. Wang, P. Chen and X.-W. Liu, *Chem. Soc. Rev.*, 2010, **39**, 2925.

95 J. Pang, P. Li, H. He, S. Xu and Z. Liu, *Chem. Sci.*, 2022, **13**, 4589.

96 A. K. Das, N. Ghosh, A. Mandal and P. C. Sil, *Biochem. Pharmacol.*, 2023, **207**, 115367.

97 Y. Choi, U. Park, H.-J. Koo, J.-S. Park, D. H. Lee, K. Kim and J. Choi, *Biosens. Bioelectron.*, 2021, **177**, 112980.

98 W.-A. Chen, Y.-H. Chen, C.-Y. Hsieh, P.-F. Hung, C.-W. Chen, C.-H. Chen, J.-L. Lin, T.-J. R. Cheng, T.-L. Hsu, Y.-T. Wu, C.-N. Shen and W.-C. Cheng, *Chem. Sci.*, 2022, **13**, 6233.

99 A. Suades, A. Qureshi, S. E. McComas, M. Coinçon, A. Rudling, Y. Chatzikyriakidou, M. Landreh, J. Carlsson and D. Drew, *Nat. Commun.*, 2023, **14**, 4070.

100 A. Ismail and M. Tanasova, *Int. J. Mol. Sci.*, 2022, **23**, 8698.

101 W. Feng, S. Zhang, Y. Wan, Z. Chen, Y. Qu, J. Li, T. D. James, Z. Pei and Y. Pei, *ACS Appl. Mater. Interfaces*, 2022, **14**, 20749.

102 S. Li, D. Zhang, Y. Li, J. Zhou, J. Chen and Y. Zhang, *Colloids Surf., B*, 2025, **252**, 114639.

103 X. Wu, Y. J. Tan, H. T. Toh, L. H. Nguyen, S. H. Kho, S. Y. Chew, H. S. Yoon and X.-W. Liu, *Chem. Sci.*, 2017, **8**, 3980.

104 Z. Luo, Y. Huang, N. Batra, Y. Chen, H. Huang, Y. Wang, Z. Zhang, S. Li, C.-Y. Chen, Z. Wang, J. Sun, Q. J. Wang, D. Yang, B. Lu, J. F. Conway, L.-Y. Li, A.-M. Yu and S. Li, *Nat. Commun.*, 2024, **15**, 255.

105 P. Kesharwani, R. Chadar, A. Sheikh, W. Y. Rizg and A. Y. Safhi, *Front. Pharmacol*, 2022, **12**, 800481.

106 Q. Guo, C. Yang and F. Gao, *FEBS J.*, 2022, **289**, 7970.

107 Z. Yaghobi, A. Movassaghpour, M. Talebi, M. A. Shadbad, K. Hajiasgharzadeh, S. Pourvahdani and B. Baradaran, *Eur. J. Pharmacol.*, 2021, **903**, 174147.

108 M. C. Nielsen, R. H. Gantzel, J. Clària, J. Trebicka, H. J. Møller and H. Grønbæk, *Cells*, 2020, **9**, 1175.

109 Z. Chen, J. Wu, L. Wang, H. Zhao and J. He, *Med. Oncol.*, 2022, **39**, 83.

110 W. Yao, H. Xu, Y. Chen, Y. Xu, F. Zhou, Z. Wang and X. Cai, *J. Drug Deliv. Sci. Technol.*, 2022, **74**, 103551.

111 C. Hou, N. Ma, Z. Shen, G. Chi, S. Chao, Y. Pei, L. Chen, Y. Lu and Z. Pei, *Int. J. Nanomed.*, 2020, **15**, 10417.

112 J. K. Elter, F. Sedlák, T. Palušák, N. Bernardová, V. Lobaz, E. Tihlaříková, V. Neděla, P. Šácha and M. Hrubý, *Biomacromolecules*, 2025, **26**, 861.

113 R. S. Wallis, A. O'Garra, A. Sher and A. Wack, *Nat. Rev. Immunol.*, 2023, **23**, 121.

114 D. Ramamurthy, T. Nundalall, S. Cingo, N. Mungra, M. Karaan, K. Naran and S. Barth, *Immunother. Adv.*, 2020, **1**, 1.

115 C. Liu, M. Yang, D. Zhang, M. Chen and D. Zhu, *Front. Immunol.*, 2022, **13**, 961805.

116 S. L. Gupta, S. Basu, V. Soni and R. K. Jaiswal, *Mol. Biol. Rep.*, 2022, **49**, 9903.

117 W.-P. Su, L.-C. Chang, W.-H. Song, L.-X. Yang, L.-C. Wang, Z.-C. Chia, Y.-C. Chin, Y.-S. Shan, C.-C. Huang and C.-S. Yeh, *ACS Appl. Mater. Interfaces*, 2022, **14**, 24144.

118 M. Pei, R. Xu, C. Zhang, X. Wang, C. Li and Y. Hu, *Colloids Surf., B*, 2021, **197**, 111378.

119 S.-u. Hassan, A. Donia, U. Sial, X. Zhang and H. Bokhari, *Pathogens*, 2020, **9**, 694.

120 S. Behren and U. Westerlind, *Eur. J. Org Chem.*, 2023, **26**, e202200795.

121 Z. Guo, J.-X. He, S. H. Mahadevegowda, S. H. Kho, M. B. Chan-Park and X.-W. Liu, *Adv. Healthcare Mater.*, 2020, **9**, 2000265.

122 D. C. Rees, E. Johnson and O. Lewinson, *Nat. Rev. Mol. Cell Biol.*, 2009, **10**, 218.

123 X. Wei, H. Sun, Y. Bai, Y. Zhang, Z. Ma, J. Li and X. Zhang, *Biomater. Sci.*, 2020, **8**, 6912.

124 F. Cui, X. Shen, B. Cao, H. Ji, J. Liu, X. Zhuang, C. Zeng, B. Qu, S. Li, Y. Xu and Q. Zhou, *Biosens. Bioelectron.*, 2022, **203**, 114044.

125 S. H. Zadeh, S. Kashanian and M. Nazari, *Biosensors*, 2023, **13**, 619.

126 Y. Zeng, F. Tang, W. Shi, Q. Dong and W. Huang, *Curr. Opin. Biotechnol.*, 2022, **74**, 247.

127 X. Chen, *Acc. Chem. Res.*, 2024, **57**, 234.

128 W. Yao and X.-S. Ye, *Acc. Chem. Res.*, 2024, **57**, 1577.

129 S. Liu, H. Yang, X. Heng, L. Yao, W. Sun, Q. Zheng, Z. Wu and H. Chen, *ACS Appl. Mater. Interfaces*, 2024, **16**, 35874.

130 M. Wojtkiewicz, S. P. Subramanian and R. L. Gundry, *Anal. Chem.*, 2024, **96**, 5746.

131 A.-L. Marie, S. Ray and A. R. Ivanov, *Nat. Commun.*, 2023, **14**, 1618.

132 C. K. Tsui, N. Twells, J. Durieux, E. Doan, J. Woo, N. Khosrojerdi, J. Brooks, A. Kulepa, B. Webster, L. K. Mahal and A. Dillin, *Nat. Commun.*, 2024, **15**, 9970.

133 Y. Miao, L. Li, Y. Wang, J. Wang, Y. Zhou, L. Guo, Y. Zhao, D. Nie, Y. Zhang, X. Zhang and Y. Gan, *Nat. Commun.*, 2024, **15**, 1159.

134 A. Piloni, C. K. Wong, F. Chen, M. Lord, A. Walther and M. H. Stenzel, *Nanoscale*, 2019, **11**, 23259.

135 S. Wan, P. M. Kelly, E. Mahon, H. Stöckmann, P. M. Rudd, F. Caruso, K. A. Dawson, Y. Yan and M. P. Monopoli, *ACS Nano*, 2015, **9**, 2157.

136 C. Cumin, L. Gee, T. Litfin, R. Muchabaiwa, G. Martin, O. Cooper, V. Heinzelmann-Schwarz, T. Lange, M. von Itzstein, F. Jacob and A. Everest-Dass, *Anal. Chem.*, 2024, **96**, 11163.

137 C. T. McDowell, Z. Klamer, J. Hall, C. A. West, L. Wisniewski, T. W. Powers, P. M. Angel, A. S. Mehta, D. N. Lewin, B. B. Haab and R. R. Drake, *Mol. Cell. Proteomics*, 2021, **20**, 100012.

138 Z. Yang, H. Tian, X. Chen, B. Li, G. Bai, Q. Cai, J. Xu, W. Guo, S. Wang, Y. Peng, Q. Liang, L. Xue and S. Gao, *Nat. Commun.*, 2024, **15**, 9097.

139 R. Pétremand, J. Chiffelle, S. Bobisse, M. A. S. Perez, J. Schmidt, M. Arnaud, D. Barras, M. Lozano-Rabella, R. Genolet, C. Sauvage, D. Saugy, A. Michel, A.-L. Huguenin-Bergenat, C. Capt, J. S. Moore, C. de Vito, S. I. Labidi-Galy, L. E. Kandalaft, D. D. Laniti, M. Bassani-Sternberg, G. Oliveira, C. J. Wu, G. Coukos, V. Zoete and A. Harari, *Nat. Biotechnol.*, 2025, **43**, 323.